Electronic Supplementary Material (ESI) for ChemComm.

Electronic Supplementary Information

Boronic acid as an efficient anchor group for surface modification of solid polyvinyl alcohol

Ryuhei Nishiyabu* and Ai Shimizu

Department of Applied Chemistry, Graduate School of Urban Environmental Sciences,
Tokyo Metropolitan University, Minami-ohsawa, Hachioji, Tokyo 192-0397, Japan
*Corresponding author: Dr. Ryuhei Nishiyabu (e-mail: ryuhei@tmu.ac.jp)

Experimental

Materials and methods

Unless otherwise described, reagents and solvents used for this study were commercially available and used as supplied. Polyvinyl alcohol (**PVA**, MW = 146 000–186 000; 87–89%, >99% hydrolyzed) was purchased from Aldrich. 4,4-Difluoro-8-(4'-hydroxyphenyl)-1,3,5,7-tetramethyl-4-bora-3a,4a-diaza-s-indacene and 9-(4-hydroxyphenyl)-10-phenylanthracene were synthesized by modified procedures of previously reported methods. A boronic acid-appended rhodamine dye (**2a**) was synthesized in our previous report. NMR spectra were recorded on a Bruker AVANCE-500 spectrometer using tetramethylsilane (TMS) as an internal standard (δ = 0 ppm) for ^{1}H and ^{13}C NMR measurements, and $BF_3{\cdot}OEt_2$ as an external standard (δ = 0 ppm) for ^{11}B NMR measurements. All NMR spectra were recorded at 298 K. Fast atom bombardment (FAB) mass spectra were obtained on a JEOL JMS-700 mass spectrometer and *m*-nitrobenzyl alcohol was used as a matrix. Atomospheric pressure chemical ionization (APCI) mass spectra were measured on a Bruker micrOTOF mass spectrometer. UV-vis absorption spectra and fluorescence spectra were measured on a Shimadzu UV-3600 spectrophotometer and a JASCO FP-6300 spectrofluorometer, respectively. A 10 mm × 10 mm quart cell was used for measuring UV-vis absorption and fluorescence spectra of solution samples. Fluorescence quantum yields of synthesized dyes were determined using fluoresceine, 9,10-diphenylanthracene and rhodamine B as reference standards. For fluorescence measurements of microparticles, a 1 mm × 10 mm quart cell was filled with microparticles and excited at 30 degrees incident angle. Fluorescence quantum yields of films were measured using a JASCO FP-8500 spectrofluorometer equipped with a substandard light source (JASCO ESC-842) and an integrating sphere (JASCO IL835). Elemental analysis was performed on an Exeter Analytical, Inc. CE-440F elemental analyzer. Field-emission scanning electron microscopy (FE- SEM) was measured by a JEOL JSM-7500F (acceleration voltage of 5 kV). For FE-SEM measurements, specimens were coated with osmium by a Meiwafosis Neoc-Pro osmium coater. Digital photographs of samples were taken with a PENTAX K-m digital camera. Fluorescence microscope images were taken using a Nikon ECLIPCE Ti equipped with a mercury lamp and a Plan Fluor 10X oil objective lens. Confocal laser scanning microscopy (CLSM) was conducted with a Nikon A1R system equipped with a Plan Apo 10X objective lens and a Plan Apo 100X oil objective lens. Solid-state ^{13}C cross-polarization-magic angle spinning (CP MAS) NMR (100 MHz) spectra were measured by a JEOL ECA 400 spectrometer. The spectrometer is equipped with a 3.2 mm MAS probehead capable of producing an MAS speed of 6 kHz. Spectra were obtained using a ^{1}H–^{13}C CP with a contact time of 2 ms, an acquisition time of 50.9 ms, a relaxation delay of 5 s between scans. The chemical shifts were calibrated using adamantine (δ = 29.5 ppm) as an external standard relative to TMS (δ = 0 ppm). X-ray photoelectron spectra (XPS) were acquired using a JEOL JPS- 9010MX. Fourier transform infrared (FT-IR) spectra were recorded on a JASCO FT/IR-4100 spectrometer equipped with an attenuated total reflection (ATR) apparatus. Electrospinning was performed by a MECC NANON electrospinning equipment.

Synthesis

To evaluate the availability of boronic acid as an anchoring group for surface modification of solid **PVA**, we decided to synthesize a series of fluorescent boronic acids because fluorescent molecules allowed for the detection of adsorption behaviours by means of not only UV-vis absorption spectroscopy but also fluorescence spectroscopy. In this study, a phenylboronic acid group was attached to three reliable fluorophores of borondipyrromethene, rhodamine, and diphenylanthracene, respectively (Fig S1). A boronic-acid appended borondipyrromethene (**1a**) was synthesized by a nucleophilic substitution reaction of 4,4-difluoro-8-(4'-hydroxyphenyl)-1,3,5,7-tetramethyl-4-bora-3a,4a-diaza-s-indacene with 3-(bromomethyl)phenylboronic acid. UV-vis absorption spectrum of **1a** showed an absorption band at 498 nm with a molar extinction coefficient of 8.8×10^4 L mol^{-1} cm^{-1} in methanol. The fluorescence spectrum of **1a** showed a peak at 506 nm with green emission in methanol and the quantum yield was determined to be 0.60. A boronic acid-appended rhodamine (**2a**) synthesized in our previous report exhibited an absorption band at 561 nm with a molar extinction coefficient of 1.3×10^5 L mol^{-1} cm^{-1} and red emission at 577 nm with a fluorescence quantum yield of 0.36 in methanol. A nucleophilic substitution reaction of 9-(4-hydroxyphenyl)-10-phenylanthracene with 3-(bromomethyl)phenylboronic acid afforded a boronic acid-appended diphenylanthracene (**3a**). The UV-vis absorption spectrum of **3a** showed absorption bands at 353 nm, 372 nm and 391 nm with a molar extinction coefficient of 1.2×10^4 L mol^{-1} cm^{-1} at 372 nm. Compound **3a** exhibited blue emission at 433 nm in methanol. The fluorescence quantum yield was determined to be 0.82. As control dyes, boronic acid-free dyes with borondipyrromethene (**1b**), rhodamine (**2b**) and diphenylanthracene (**3b**) fluorephores were synthesized in the same manners and exhibited similar optical properties to the corresponding boronic acid-appended dyes, respectively.

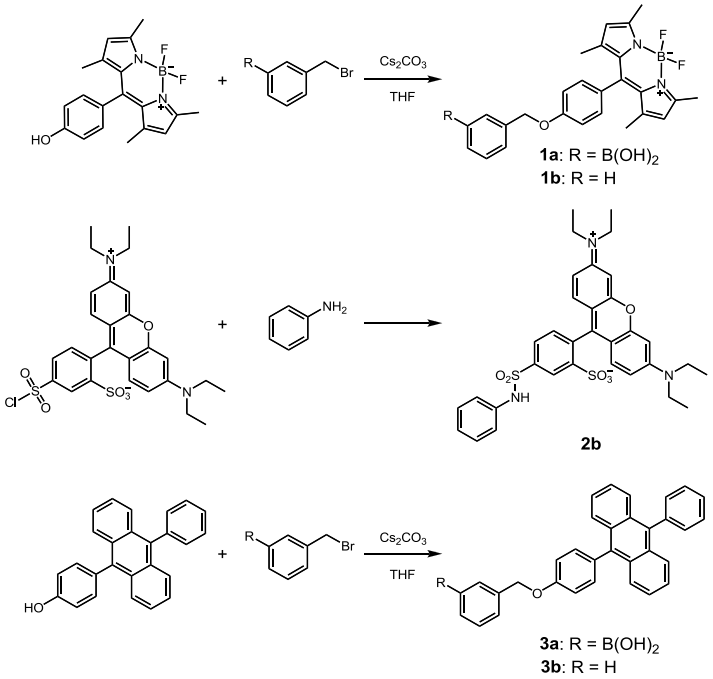

Fig. S1 Synthesis of **1a**, **1b**, **2b**, **3a** and **3b**.

*Synthesis of boronic acid-appended borondipyrromethene **1a***. 4,4-Difluoro-8-(4'-hydroxyphenyl)-1,3,5,7-tetramethyl-4-bora-3a,4a-diaza-s-indacene (0.30 g, 0.88 mmol) was dissolved in dry THF (30 mL). Cesium carbonate (1.44 g, 4.4 mmol) was added to the solution followed by the addition of 3-(bromomethyl)phenylboronic acid (0.22 g, 1.0 mmol) under a nitrogen atmosphere. The resultant mixture was stirred at room temperature for 6 h, and then the solvent was removed *in vacuo*. The residue was dissolved in dichloromethane (100 mL) and water (100 mL) was added to the solution. After neutralization of the aqueous layer by adding hydrochloric acid, the organic layer was collected. The organic layer was dried over anhydrous sodium sulfate and the solvent was removed *in vacuo*. The crude product was chromatographed on silica gel (wako gel C-300) using 1% methanol in dichloromethane as an eluent. In this way, 0.40 g of **1a** was obtained as an orange solid (96% yield). UV-vis: λ_{max} = 498 nm (ε = 8.8 × 10^4 L mol^{-1} cm^{-1}) in methanol. FL: λ_{em} = 506 nm (Φ = 0.60) in methanol. ^{1}H NMR (500 MHz, DMSO-d_6): δ/ppm 1.40 (s, 6H), 2.50 (s, 6H), 5.16 (s, 2H), 6.17 (s, 2H), 7.20 (d, *J* = 8.7 Hz, 2H), 7.27 (d, *J* = 8.6 Hz, 2H), 7.37 (t, *J* = 7.5 Hz, 1H), 7.51 (d, *J* = 7.6 Hz, 1H), 7.77 (d, *J* = 7.4 Hz, 1H), 7.89 (s, 1H), 8.08 (s, 2H). ^{13}C NMR (125 MHz, DMSO-d_6): δ/ppm 14.6, 70.3, 116.1, 121.7, 126.6, 127.9, 129.6, 130.2, 131.6, 134.2, 134.4, 135.9, 142.6, 143.2, 155.1, 159.5. ^{11}B NMR (160 MHz, DMSO-d_6): δ/ppm 0.60 (t, *J* = 31.5 Hz), 29.80 (s). MS (FAB^+) *m*/*z* = 744 [**1a** + 2(*m*-nitrobenzylalcohol) − $2H_2O$]+. Elemental analysis: calc. for $C_{26}H_{26}B_2F_2N_2O_2 \cdot 0.25CH_2Cl_2$: C, 63.65; H, 5.39; N, 5.66%, found: C, 63.74; H, 5.46; N, 5.46%.

*Synthesis of 4,4-difluoro-8-(4'-benzyloxyphenyl)-1,3,5,7-tetramethyl-4-bora-3a,4a-diaza-s-indacene **1b***. 4,4-Difluoro-8-(4'-hydroxyphenyl)-1,3,5,7-tetramethyl-4-bora-3a,4a-diaza-s-indacene (0.40 g, 1.2 mmol) was dissolved in dry THF (30 mL). Cesium carbonate (1.74 g, 5.3 mmol) was added to the solution followed by the addition of benzyl bromide (0.18 g, 1.1 mmol) under a nitrogen atmosphere. The resultant mixture was stirred at room temperature overnight. Insoluble solids in the mixture were removed by filtration and the resultant solution was concentrated *in vacuo*. The crude product was chromatographed on silica gel (wako gel C-300) using 20% hexane in dichloromethane as an eluent. In this way, 0.37 g of **1b** was obtained as an orange solid (82% yield). UV-vis: λ_{max} = 498 nm (ε = 9.0 × 10^4 L mol^{-1} cm^{-1}) in methanol. FL: λ_{em} = 506 nm (Φ = 0.58) in methanol. ^{1}H NMR (500 MHz, $CDCl_3$): δ/ppm 1.43 (s, 6H), 2.55 (s, 6H), 5.13 (s, 2H), 5.97 (s, 2H), 7.09 (d, *J* = 8.3, 2H), 7.18 (d, *J* = 8.3 Hz, 2H), 7.35 (t, *J* = 7.2 Hz, 1H), 7.41 (t, *J* = 7.4 Hz, 2H), 7.46 (d, *J* = 7.4 Hz, 2H). ^{13}C NMR (125 MHz, $CDCl_3$): δ/ppm 14.7, 70.2, 115.6, 121.1, 127.4, 127.6, 128.2, 128.6, 129.2, 131.8, 136.5, 141.8, 143.2, 155.3, 159.3. ^{11}B NMR (160 MHz, $CDCl_3$): δ/ppm 0.79 (t, *J* = 33.3 Hz). MS ($APCI^+$) *m*/*z* = 430 [**1b**]$^+$. Elemental analysis: calc. for $C_{26}H_{25}BF_2N_2O$: C, 72.57; H, 5.86; N, 6.51%, found: C, 72.29; H, 5.76; N, 6.43%.

*Synthesis of 2-(3-diethylamino-6-diethylazaniumylidene-xanthen-9-yl)-5-(aminophenulsulfonyl)-benzenesulfonate **2b***. Lissamine rhodamine B sulfonyl chloride (187 mg, 0.32 mmol) was added to distilled aniline (5 mL) under a nitrogen atmosphere and the resultant mixture was stirred at room

temperature for 23 h. Chloroform (100 mL) was added to the mixture and washed with 1 M hydrochloric acid. The organic layer was collected and dried over anhydrous sodium sulfate. The resultant solution was concentrated *in vacuo* and the residue was chromatographed on silica gel (wako gel C-300) using 5% methanol in chloroform as an eluent. In this way, 66 mg of **2b** was obtained as a dark green solid (32% yield). UV-vis: λ_{max} = 561 nm ($\varepsilon = 1.3 \times 10^5$ L mol^{-1} cm^{-1}) in methanol. FL: λ_{em} = 577 nm (Φ = 0.42) in methanol. ^{1}H NMR (500 MHz DMSO-d_6): δ/ppm 1.20 (t, *J* = 7.0 Hz, 12H), 3.63 (m, 8H), 6.85 (d, *J* = 9.6 Hz, 2H), 6.92 (d, *J* = 2.4 Hz, 2H), 7.04 (dd, *J* = 2.4, 7.9 Hz, 2H), 7.10 (t, *J* = 7.3 Hz, 2H), 7.16 (dd, *J* = 1.0, 8.5 Hz, 2H), 7.31 (t, *J* = 7.9 Hz, 2H), 7.40 (d, *J* = 8.0 Hz, 1H), 7.81 (dd, *J* = 1.9, 8.8 Hz, 1H), 8.47 (d, *J* = 1.9 Hz, 1H), 10.53 (s, 1H). ^{13}C NMR (125 MHz, DMSO-d_6): δ/ppm 12.5, 45.2, 95.4, 113.4, 113.7, 120.6, 124.5, 125.9, 126.7, 129.3, 130.6, 132.5, 133.5, 137.4, 140.6, 148.2, 155.0, 157.1. MS (FAB$^+$) *m*/*z* 634 [**2b** + H]$^+$. Elemental analysis: calc. for $C_{33}H_{35}N_3O_6S_2$: C, 62.53; H, 5.57; N, 6.63%, found: C, 62.14; H, 5.26; N, 6.53%.

*Synthesis of boronic acid-appended diphenylanthracene **3a***. 9-(4-Hydroxyphenyl)-10-phenylanthracene (0.25 g, 0.72 mmol) was dissolved in dry THF (30 mL). Cesium carbonate (1.18 g, 3.61 mmol) was added to the solution followed by the addition 3-(bromomethyl)phenylboronic acid (0.18 g, 0.82 mmol) in a nitrogen atmosphere. The resultant mixture was stirred at room temperature for 5 h. Then the solvent was removed *in vacuo* and dichloromethane (100 mL) and water (100 mL) were added to the residue. After the aqueous layer was neutralized by adding hydrochloric acid, the organic layer was collected and dried over anhydrous sodium sulfate. Concentration of the solution afforded **3a** as a white precipitate (0.31 g, 89% yield). UV-vis: λ_{max} = 353 nm, 372 nm and 391 nm ($\varepsilon = 1.2 \times 10^4$ L mol^{-1} cm^{-1} at 372 nm) in methanol. FL: λ_{em} = 433 nm (Φ = 0.82) in methanol. ^{1}H NMR (500 MHz, DMSO-d_6): δ/ppm 5.25 (s, 2H), 7.30 (d, *J* = 8.8 Hz, 2H), 7.47-7.38 (m, 9H), 7.68-7.56 (m, 8H), 7.81 (d, *J* = 7.4 Hz, 2H), 7.98 (s, 1H), 8.11 (s, 2H). ^{13}C NMR (125 MHz, DMSO-d_6): δ/ppm 69.8, 114.9, 125.39, 125.5, 126.4, 126.5, 127.6, 127.8, 128.7, 129.2, 129.5, 129.7, 130.2, 130.9, 132.1, 133.75, 133.83, 135.9, 136.4, 136.5, 138.2, 158.1. ^{11}B NMR (160 MHz, DMSO-d_6): δ/ppm 30.43 (s). MS (FAB$^+$) *m*/*z* = 750 [**3a** + 2(*m*-nitrobenzylalcohol) − 2H$_2$O]$^+$. Elemental analysis: calc. for $C_{33}H_{35}BO_3 \cdot 0.25CH_2Cl_2$: C, 79.62; H, 5.12%, found: C, 79.63; H, 4.95%.

*Synthesis of 9-(4-benzyloxyphenyl)-10-phenylanthracene **3b***. 9-(4-Hydroxyphenyl)-10-phenylanthracene (0.10 g, 0.29 mmol) was dissolved in dry THF (30 mL) and cesium carbonate (0.47 g, 1.44 mmol) was added to the solution followed by the addition of benzyl bromide (0.06 g, 0.35 mmol) under a nitrogen atmosphere. The resultant mixture was stirred at room temperature overnight. Insoluble solids in the mixture were removed by filtration and the resultant solution was concentrated *in vacuo*. The crude product was chromatographed on silica gel (wako gel C-300) using 10% hexane in dichloromethane as an eluent. In this way, 0.12 g of **3b** was obtained as a white solid (95% yield). UV-vis: λ_{max} = 354 nm, 372 nm and 392 nm ($\varepsilon = 1.4 \times 10^4$ L mol^{-1} cm^{-1} at 372 nm) in methanol. FL: λ_{em} = 433 nm (Φ = 0.71) in methanol. ^{1}H NMR (500 MHz, $CDCl_3$): δ/ppm 5.22 (s, 1H), 7.22 (d, *J* =

8.7 Hz, 2H), 7.35-7.31 (m, 4H), 7.42-7.37 (m, 3H), 7.49-7.44 (m, 4H), 7.56-7.53 (m, 3H), 7.62-7.59 (m, 2H), 7.70-7.67 (m, 2H), 7.77-7.74 (m, 2H). ^{13}C NMR (125 MHz, $CDCl_3$): δ/ppm 70.2, 114.8, 124.9, 125.0, 127.0, 127.1, 127.4, 127.7, 128.1, 128.4, 128.7, 129.9, 130.2, 131.3, 131.4, 132.4, 136.9, 137.0, 137.1, 139.1, 158.3. MS (APCI$^+$) *m*/*z* = 436 [**3b**]$^+$. Elemental analysis: calc. for $C_{33}H_{24}O$: C, 90.79; H, 5.54%, found: C, 90.67; H, 5.47%.

Preparation of PVA microparticles, films and nanofibers

In this study, partially hydrolyzed **PVA** (MW = 146 000–186 000; 87–89% hydrolyzed) was employed because the use of highly hydrolyzed **PVA** (MW = 146 000–186 000; 99% hydrolyzed) led to negligible adsorption of boronic acids while nanofibers of 99% hydrolyzed **PVA** showed detectable adsorption of boronic acids due to their high specific surface area.

PVA particles were screened using a screening shaker with a 425 μm sieve and a 212 μm sieve. The particles on the 212 μm sieve were collected and rinsed with methanol. The obtained particles were dried *in vacuo*. An average size of the screened particles was determined to be 405 ± 95 μm by scanning electron microscopy. For preparation of **PVA** films, **PVA** particles (2.4 g) were added to water (40 mL) and the suspension was allowed to stand at 80 °C until complete dissolution. The resultant 6% (w/v) **PVA** solution was cooled down to room temperature. The solution (10 mL) was poured into a silicone rubber frame (10 cm × 10 cm) on a glass plate at room temperature and left in a dry oven at 60 °C for 48 h. The obtained films showed a high transparency and the thickness was 76 μm. For preparation of **PVA** nanofibers, **PVA** particles (4.0 g) were added to water (40 mL) and the suspension was allowed to stand at 80 °C until complete dissolution. The resultant 10% (w/v) **PVA** solution was cooled down to room temperature and loaded into a syringe equipped with a stainless steel needle with 0.7 mm inner diameter. The needle was connected to a high-voltage supply (25 kV) and a flat plate collector was placed 15 cm apart. Then the solution was delivered with a flow rate of 0.5 mL h^{-1} and nanofibers were collected for 40 min. The thickness and average diameter of resultant nanofibers were 43 μm and 470 ± 110 nm respectively.

Chemical modification of the surface of PVA microparticles

Chemical modification of the surface of **PVA** microparticles with boronic acids was conducted by a simple soaking technique as follows. To a methanol solution of **1a** (2.0×10^{-5} M, 5 mL) in 50 mL vial was added **PVA** microparticles (50 mg). The sample was shaken at room temperature for 24 h using a shaking apparatus (80 rpm). The resultant solid was collected by filtration and rinsed with methanol. For ^{13}C CP MAS NMR, XPS and ATR-FT-IR measurements, **PVA** microparticles (50 mg) were soaked in a methanol solution of **1a** (2.6×10^{-4} M, 5 mL) for 24 h and the collected microparticles were rinsed with methanol.

Quantitative evaluation of adsorption behaviour

To methanol solutions of **1a** at varied concentrations (0 – 2.6 × 10^{-4} M, 5 mL) in 50 mL vials were added **PVA** microparticles (50 mg). The resultant samples were shaken at room temperature for 24 h using a shaking apparatus (80 rpm). Equilibrium concentrations of **1a** were determined from absorption intensities at 498 nm of the resultant solutions and the amounts of **1a** adsorbed were calculated from the equilibrium concentrations. The obtained adsorption isotherm was analyzed with the equations for a stoichiometric 1 : 1 binding mode between 1a and each diol moiety of **PVA**. According to the assumption, the amounts of **1a** adsorbed (q) was expressed in the following equations;

$$q = \frac{q_{\max} \times (\mathrm{A} - \sqrt{\mathrm{A}^2 - 4 \times K^2 \times [\mathrm{diol}]_0 \times [\mathrm{dye}]_0})}{2 \times K \times [\mathrm{diol}]_0}$$

$$\mathrm{A} = K \times [\mathrm{dye}]_0 + K \times [\mathrm{diol}]_0 + 1$$

In the equation, $q_{\max}$, K, $[\mathrm{diol}]_0$, and $[\mathrm{dye}]_0$ are a maximum adsorption capacity, an apparent association constant, an initial apparent concentration of diol moiety of **PVA** and initial concentrations of **1a**, respectively. The values of $q_{\max}$, K and $[\mathrm{diol}]_0$ were evaluated by a nonlinear least-squares method.

Functionalization of PVA films and nanofibers

Functionalization of **PVA** films and nanofibers with boronic acid-appended fluorescent dyes was typically conducted as follows. To a methanol solution of **1a** (2.0 × 10^{-5} M, 5 mL) in a 50 mL vial was added a **PVA** film (1 cm × 1 cm). The sample was shaken at room temperature for 24 h using a shaking apparatus (80 rpm). The resultant film was taken from the solution and rinsed with methanol. For functionalization of **PVA** nanofibers, a **PVA** nanofiber mat (1 cm × 1 cm) was added to a methanol solution of **1a** (2.0 × 10^{-5} M, 5 mL) in a 50 mL vial and the sample was shaken at room temperature for 24 h using a shaking apparatus (80 rpm). The resultant mat was taken from the solution and rinsed with methanol.

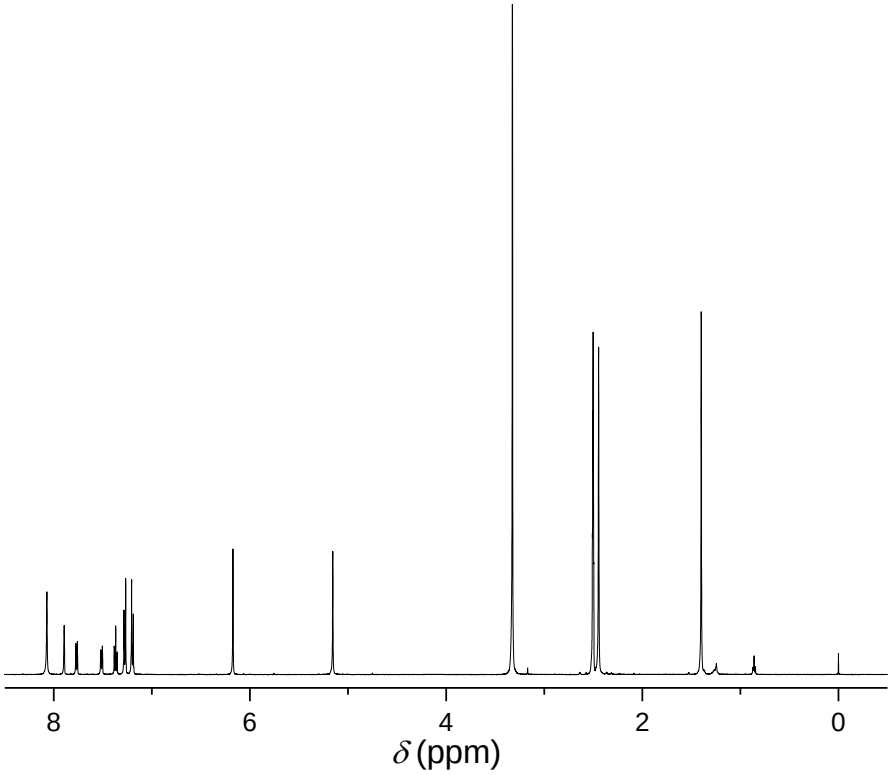

Fig. S2 ^{1}H NMR spectrum of **1a** in DMSO-d_6.

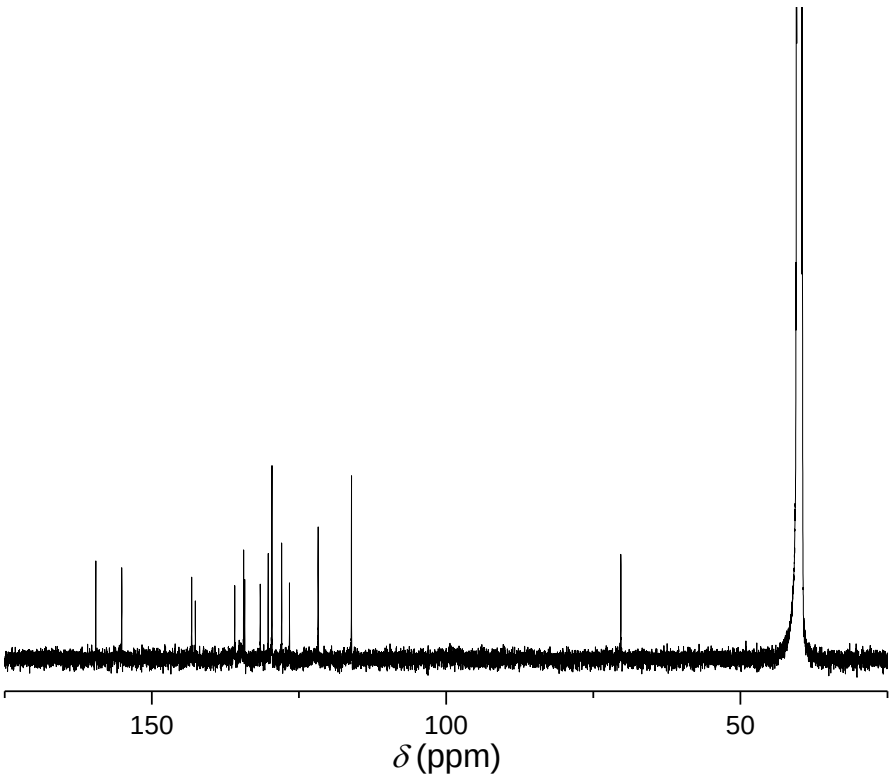

Fig. S3 ^{13}C NMR spectrum of **1a** in DMSO-d_6.

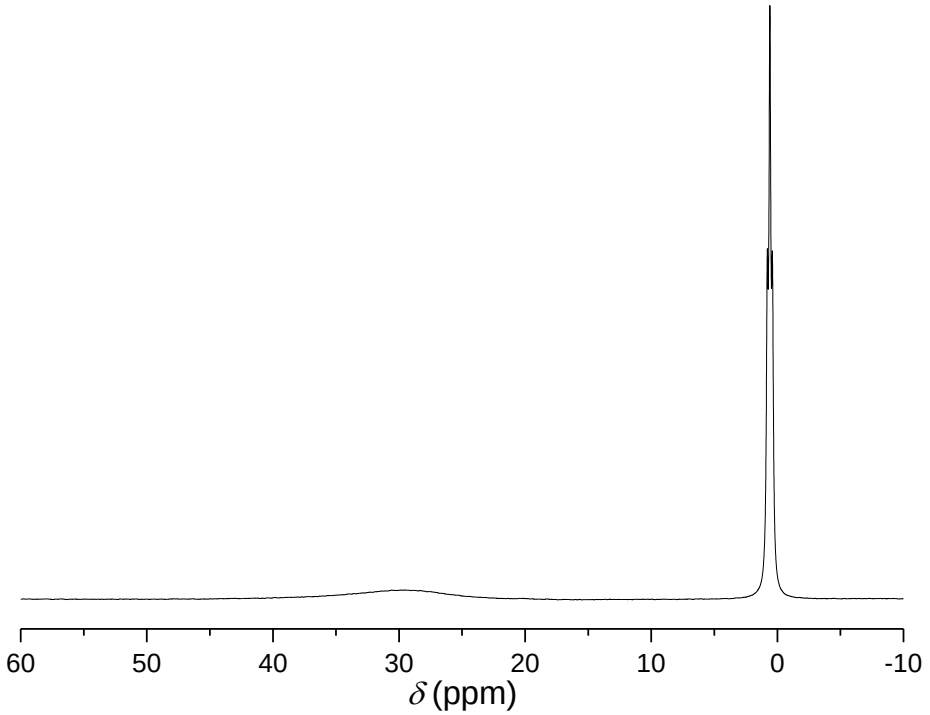

Fig. S4 ^{11}B NMR spectrum of **1a** in DMSO-d_6.

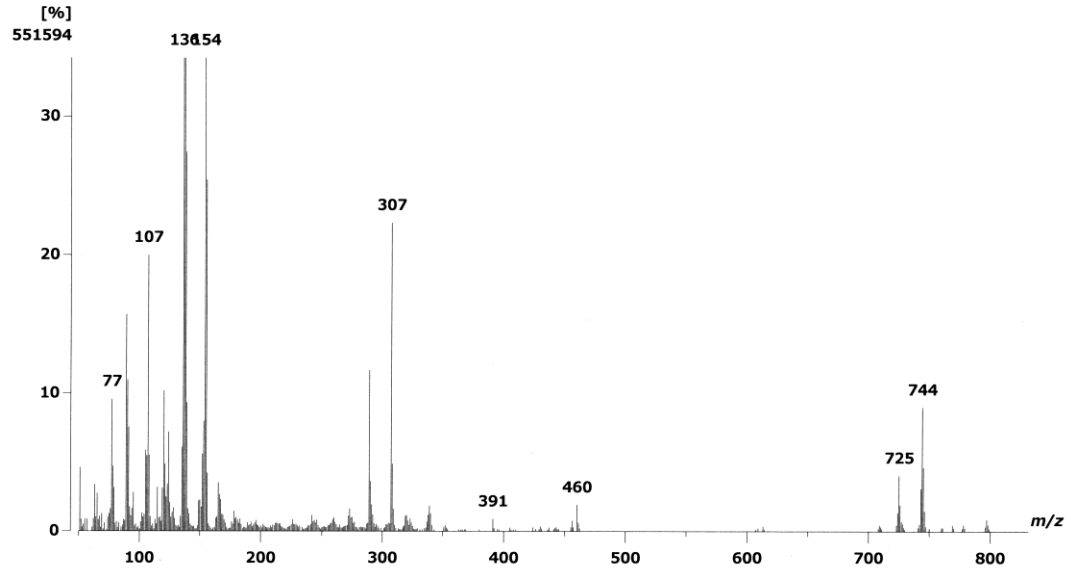

Fig. S5 FAB mass spectrum of **1a**.

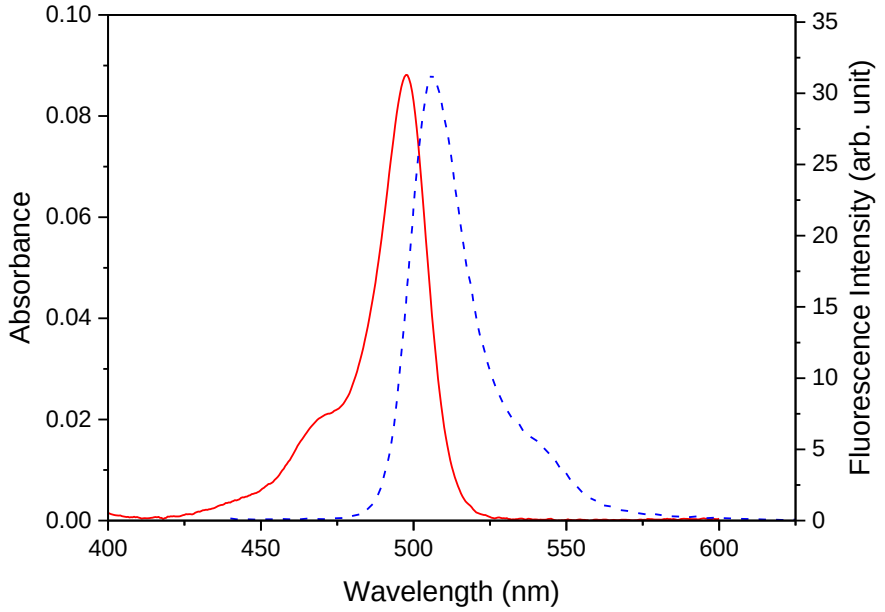

Fig. S6 UV-vis absorption (solid line) and fluorescence (dashed line) spectra of **1a** (1.0×10^{-6} M) in methanol at 20 °C. A 1 cm × 1 cm quart cell was used. λ_{ex} = 436 nm.

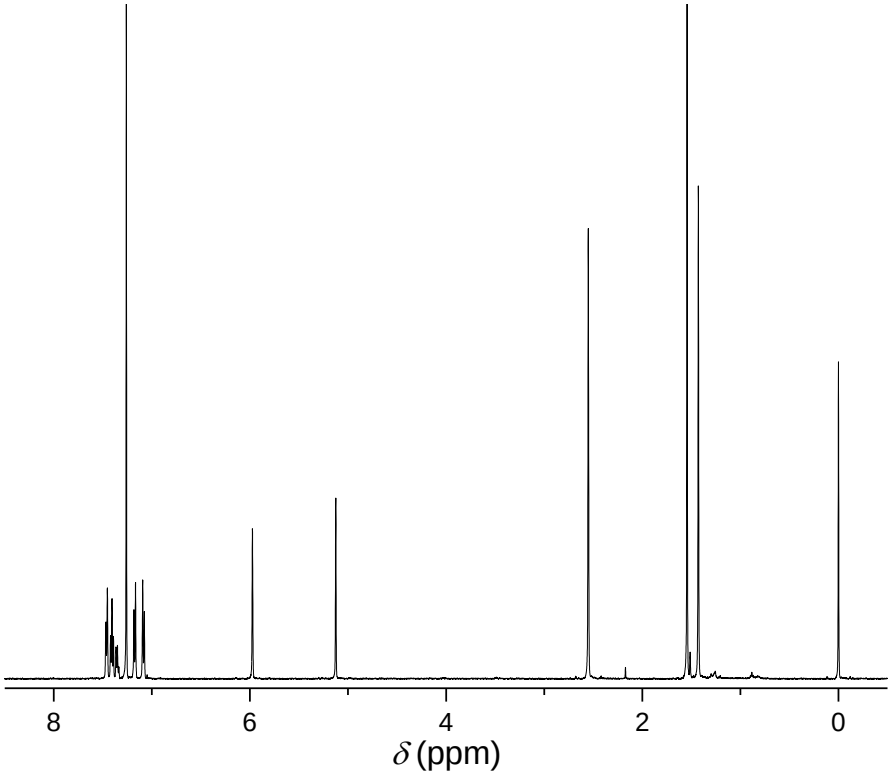

Fig. S7 ^{1}H NMR spectrum of **1b** in $CDCl_3$.

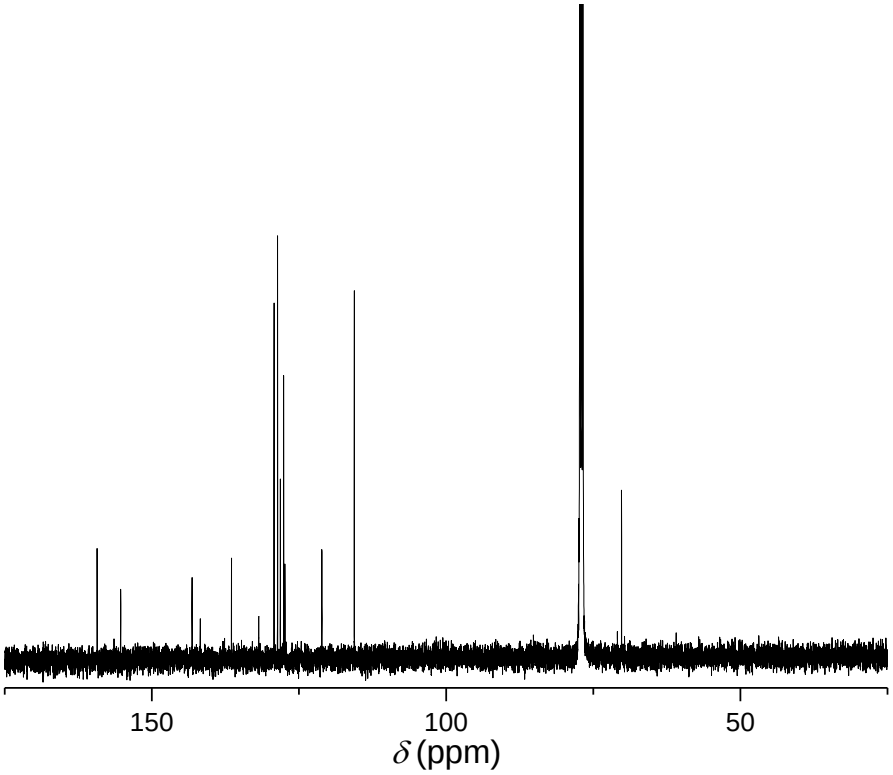

Fig. S8 ^{13}C NMR spectrum of **1b** in $CDCl_3$.

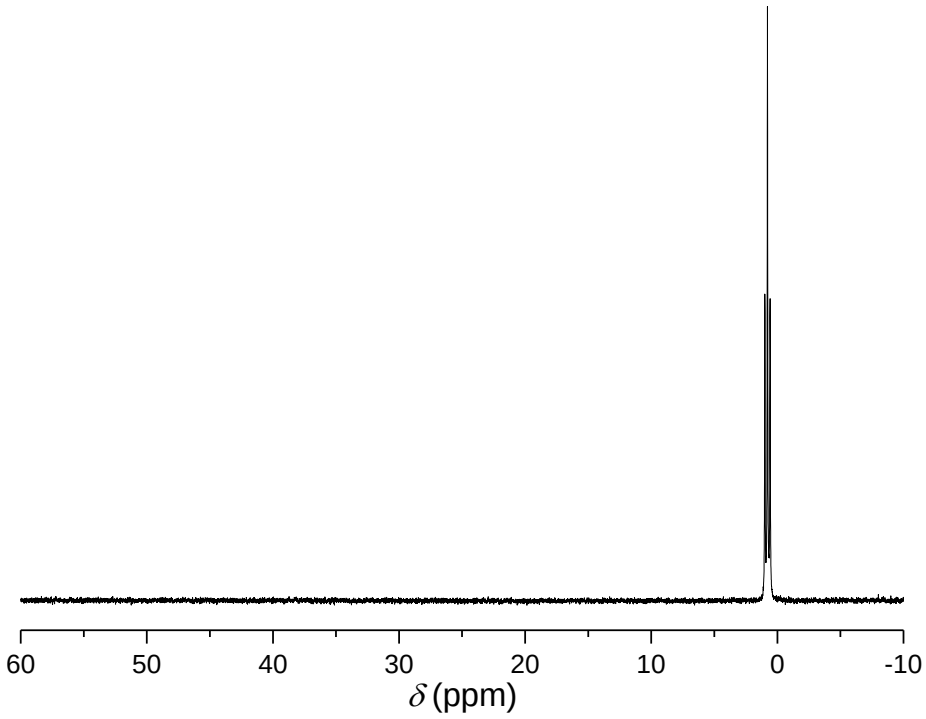

Fig. S9 ^{11}B NMR spectrum of **1b** in $CDCl_3$.

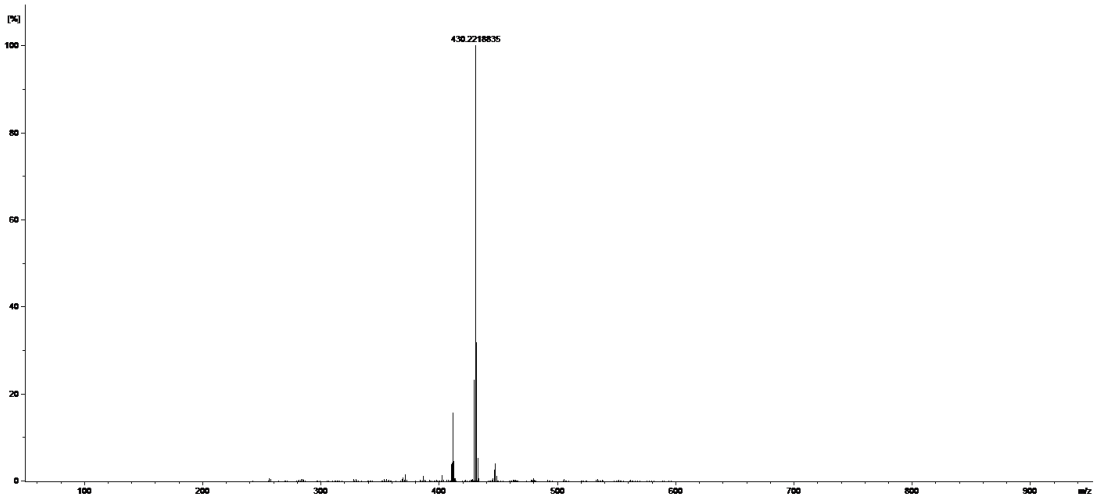

Fig. S10 APCI mass spectrum of **1b**.

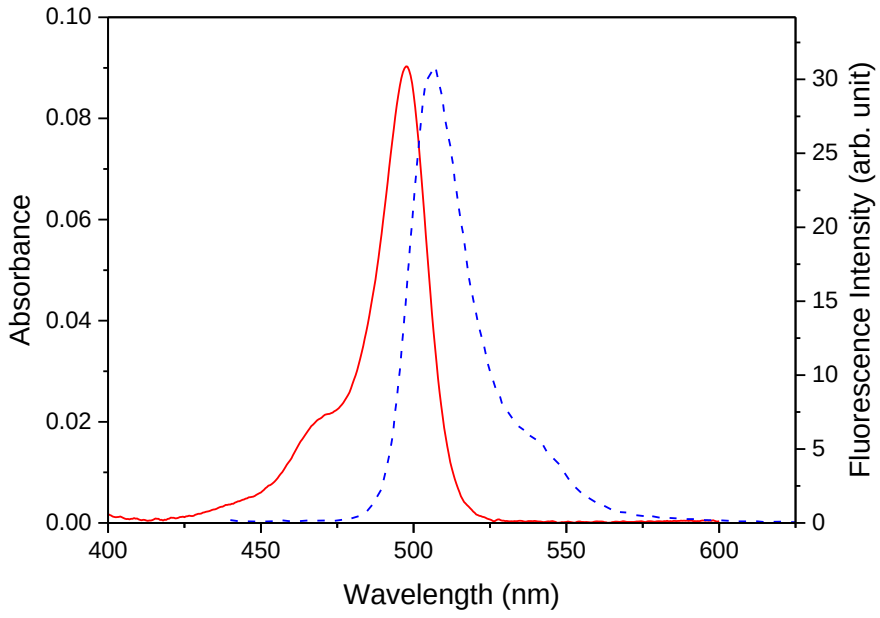

Fig. S11 UV-vis absorption (solid line) and fluorescence (dashed line) spectra of **1b** (1.0×10^{-6} M) in methanol at 20 °C. A 1 cm × 1 cm quart cell was used. λ_{ex} = 436 nm.

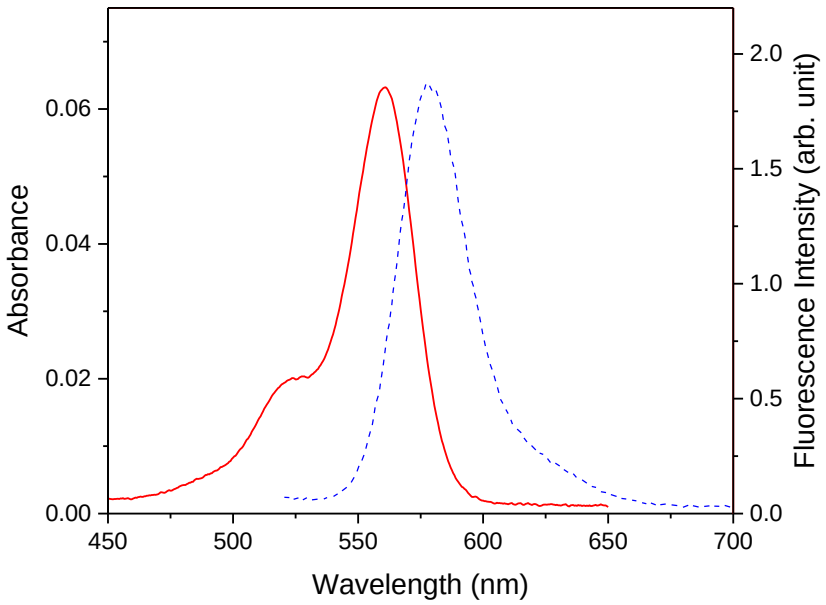

Fig. S12 UV-vis (solid line) and fluorescence (dashed line) spectra of **2a** (5.0×10^{-7} M) in methanol at 20 °C. A 1 cm × 1 cm quart cell was used. λ_{ex} = 510 nm.

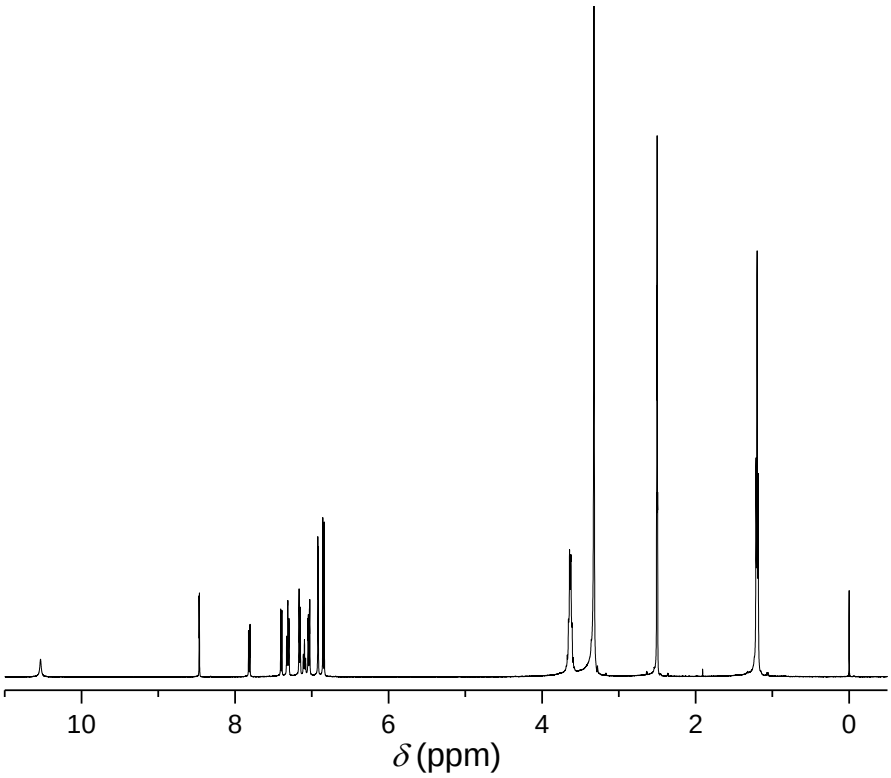

Fig. S13 ^{1}H NMR spectrum of **2b** in DMSO-d_6.

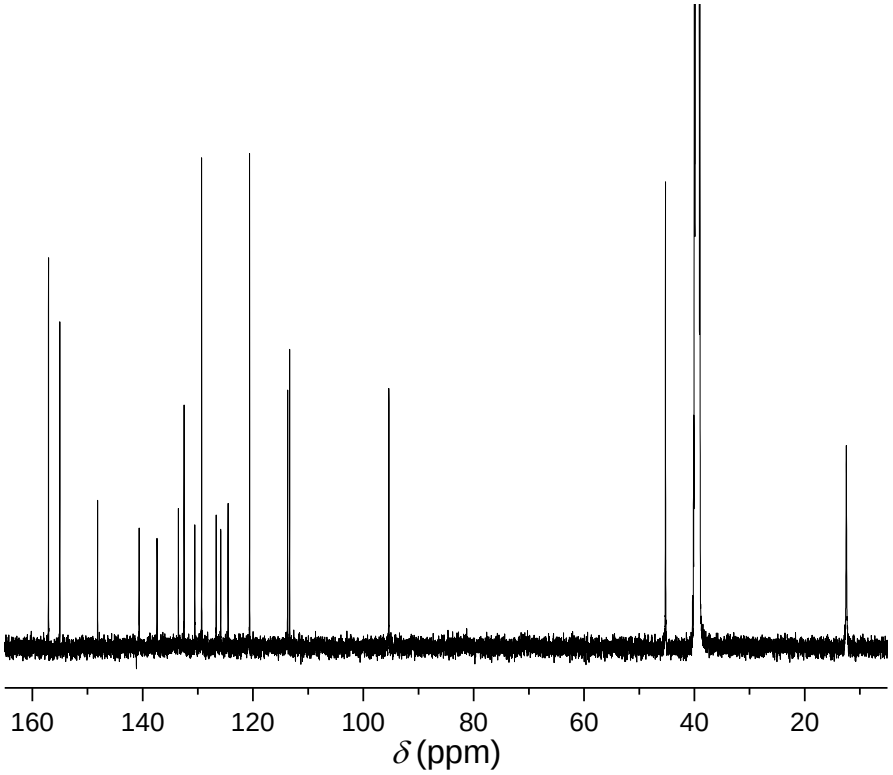

Fig. S14 ^{13}C NMR spectrum of **2b** in DMSO-d_6.

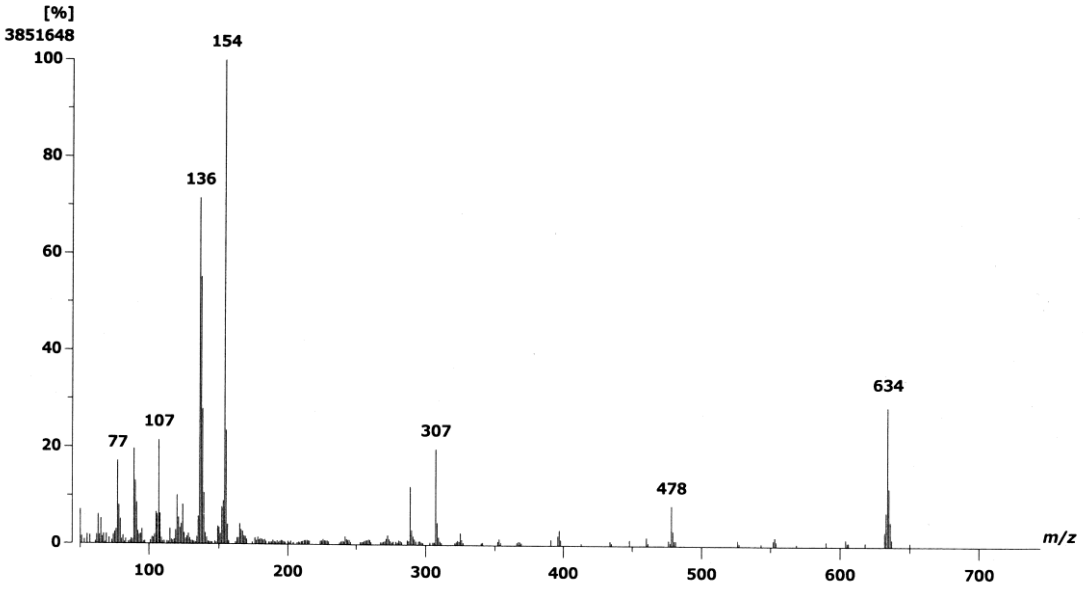

Fig. S15 FAB mass spectrum of **2b**.

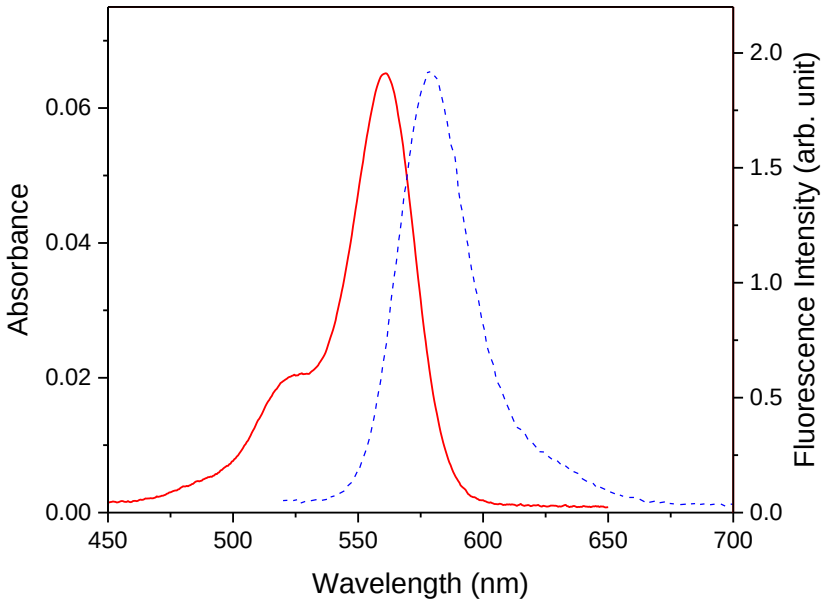

Fig. S16 UV-vis absorption (solid line) and fluorescence (dashed line) spectra of **2b** (5.0×10^{-7} M) in methanol at 20 °C. A 1 cm × 1 cm quart cell was used. λ_{ex} = 510 nm.

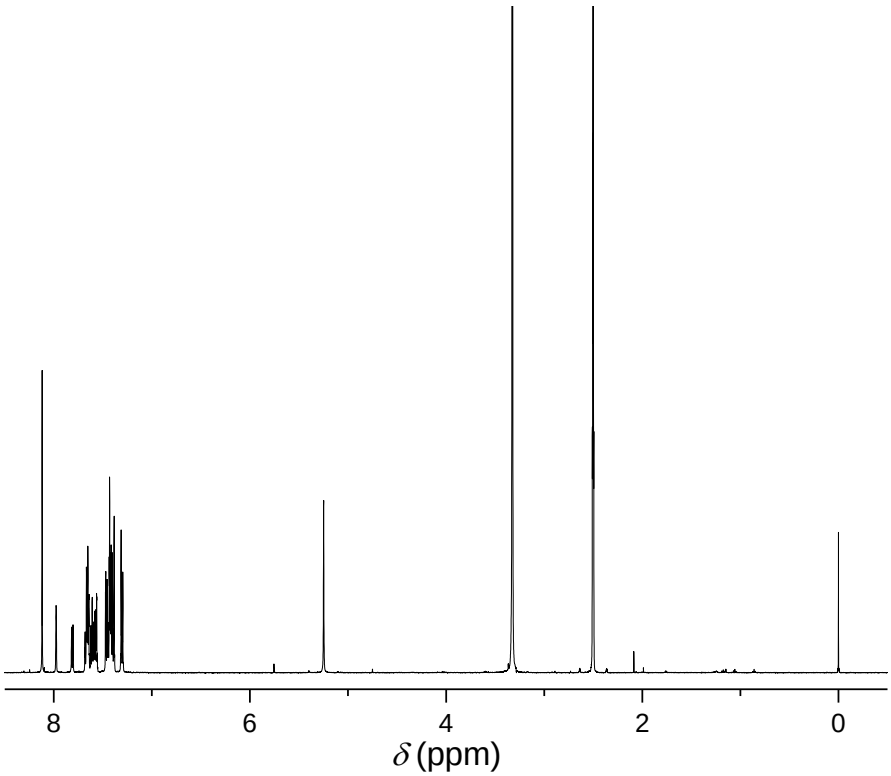

Fig. S17 ^{1}H NMR spectrum of **3a** in DMSO-d_6.

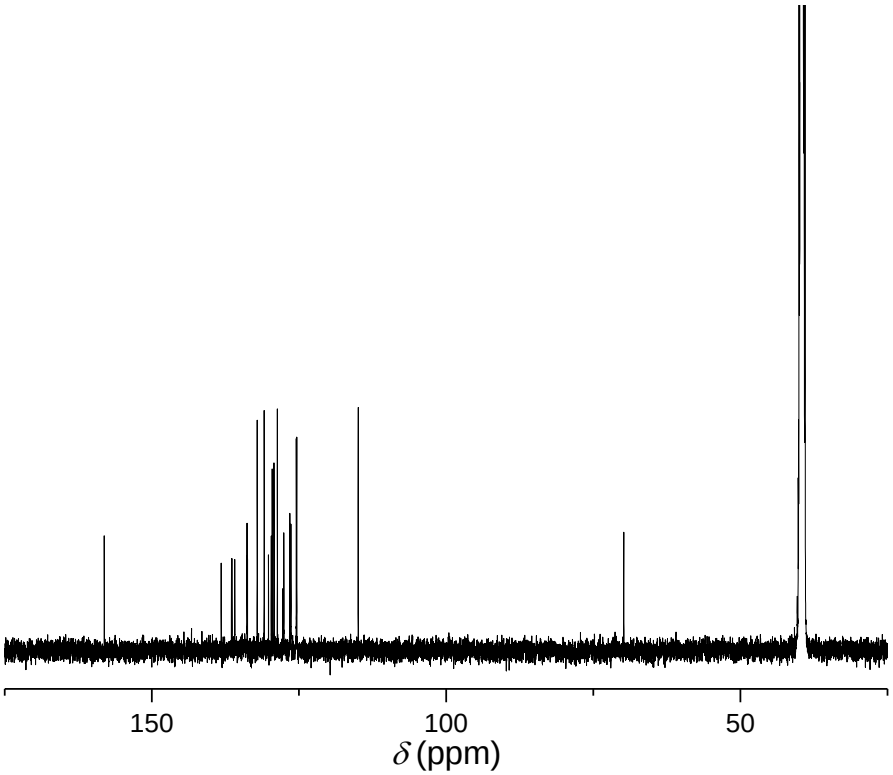

Fig. S18 ^{13}C NMR spectrum of **3a** in DMSO-d_6.

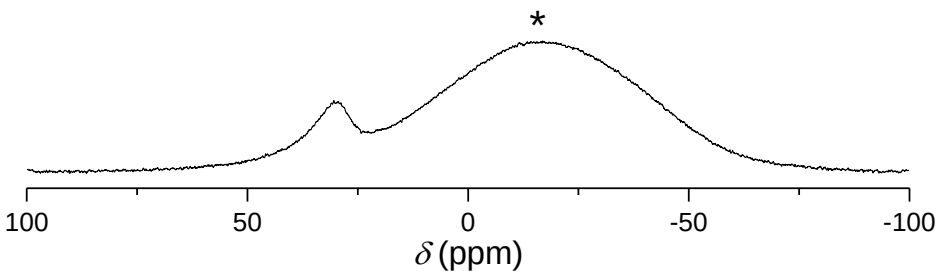

Fig. S19 ^{11}B NMR spectrum of **3a** in DMSO-d_6. A broad background peak (*) is assigned to boron nitride used in the NMR probe.

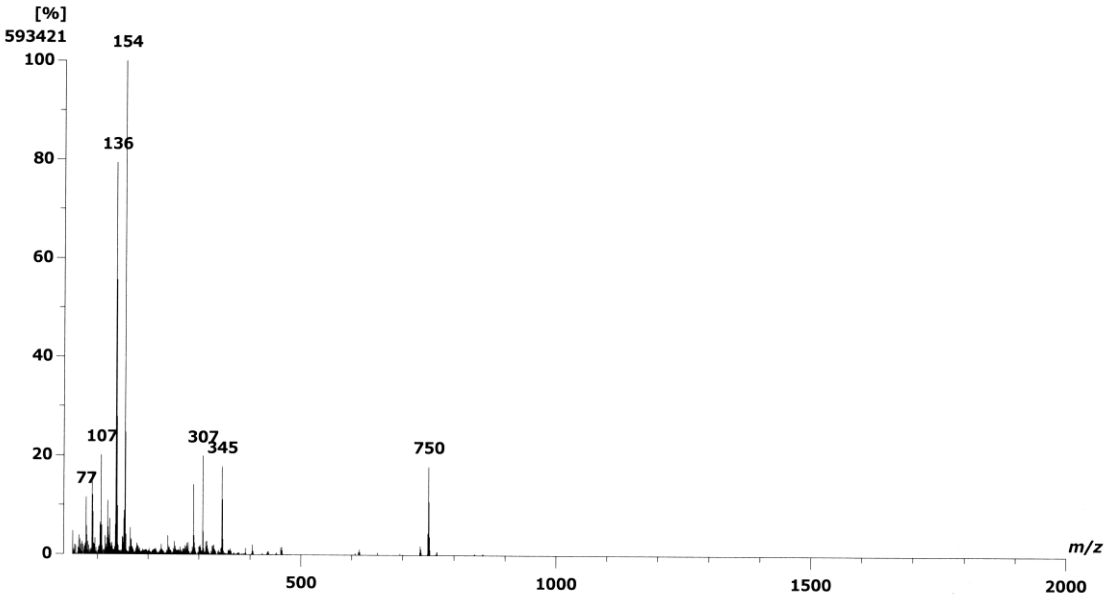

Fig. S20 FAB mass spectrum of **3a**.

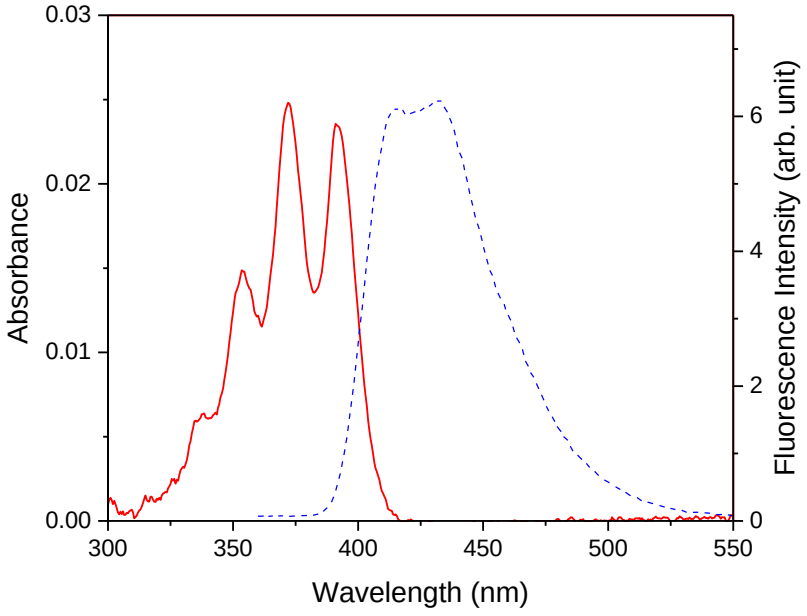

Fig. S21 UV-vis absorption (solid line) and fluorescence (dashed line) spectra of **3a** (2.0×10^{-6} M) in methanol at 20 °C. A 1 cm × 1 cm quart cell was used. λ_{ex} = 355 nm.

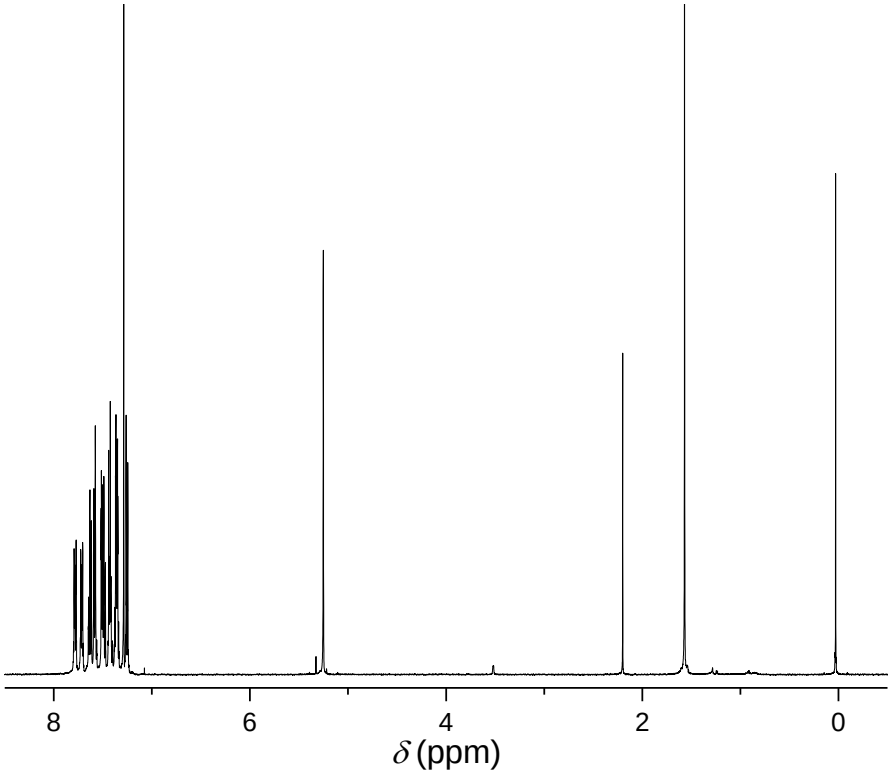

Fig. S22 ^{1}H NMR spectrum of **3b** in $CDCl_3$.

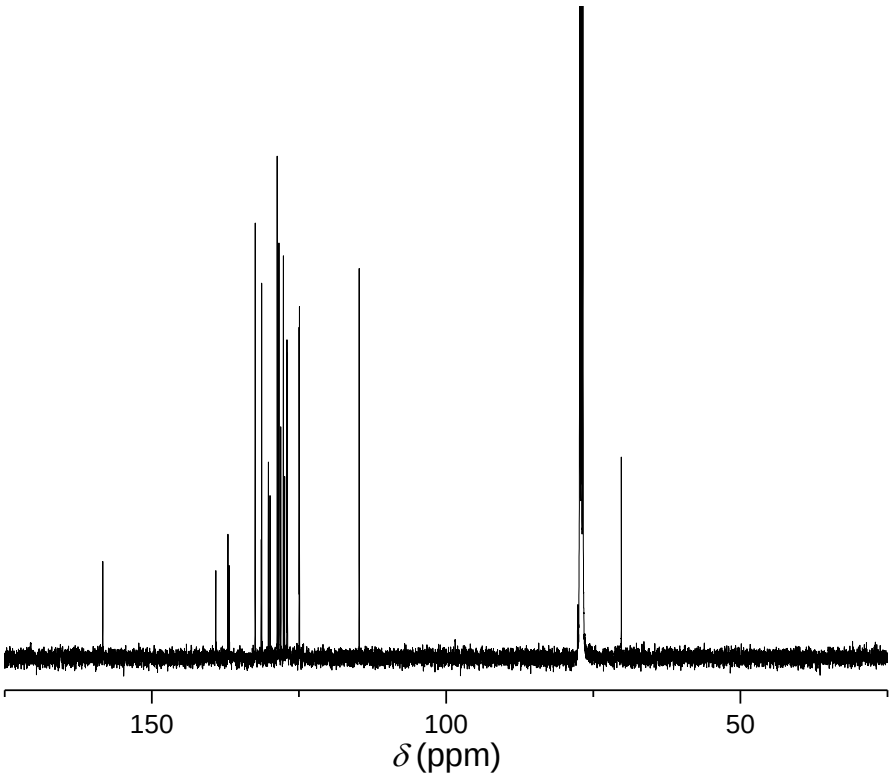

Fig. S23 ^{13}C NMR spectrum of **3b** in $CDCl_3$.

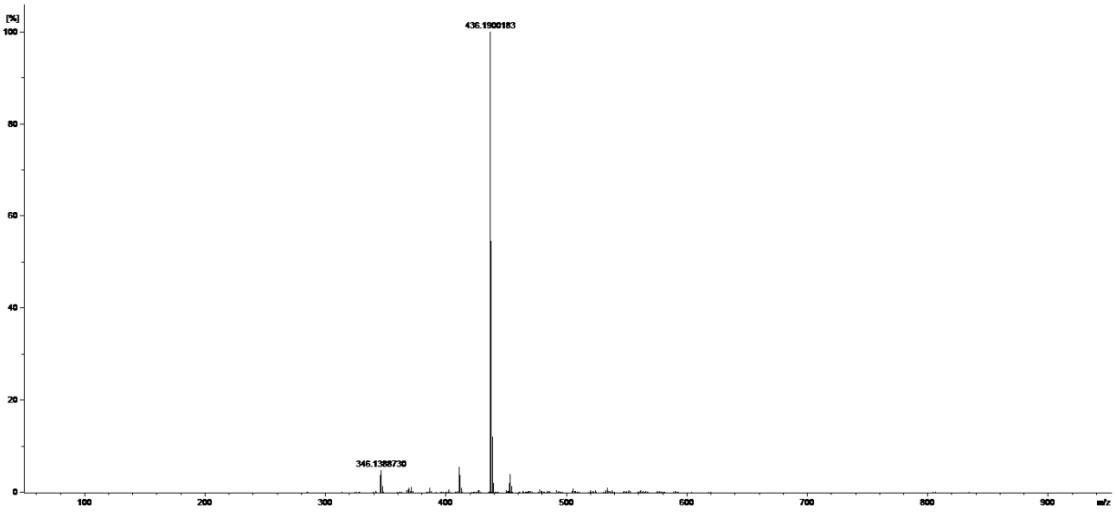

Fig. S24 APCI mass spectrum of **3b**.

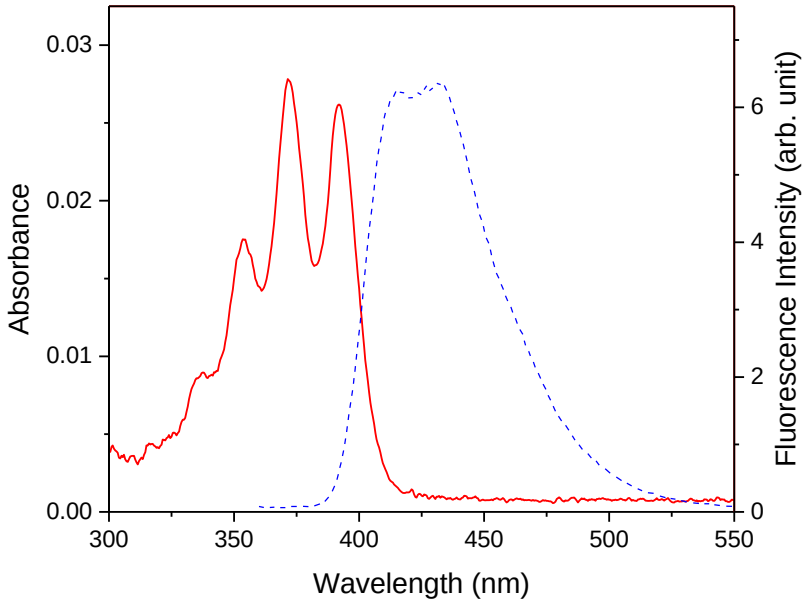

Fig. S25 UV-vis absorption (solid line) and fluorescence (dashed line) spectra of **3b** (2.0×10^{-6} M) in methanol at 20 °C. A 1 cm × 1 cm quart cell was used. λ_{ex} = 355 nm.

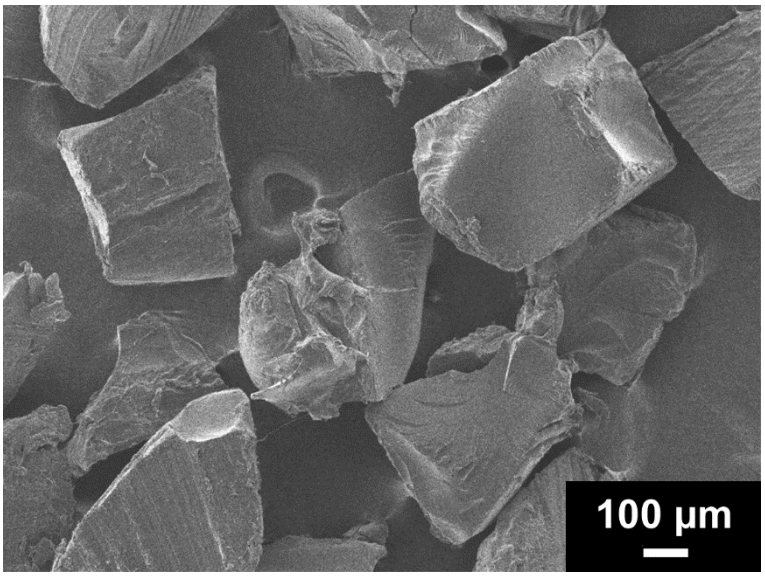

Fig. S26 FE-SEM image of **PVA** microparticles.

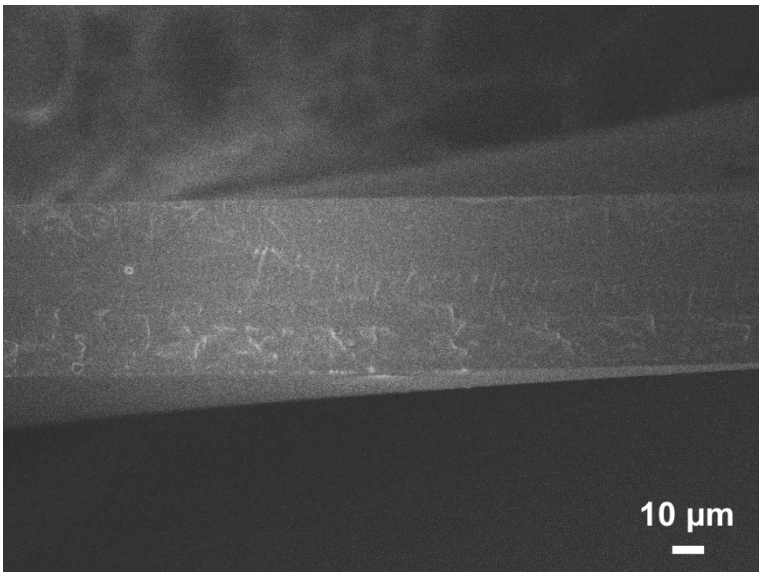

Fig. S27 Cross-sectional FE-SEM image of **PVA** film prepared by a casting technique.

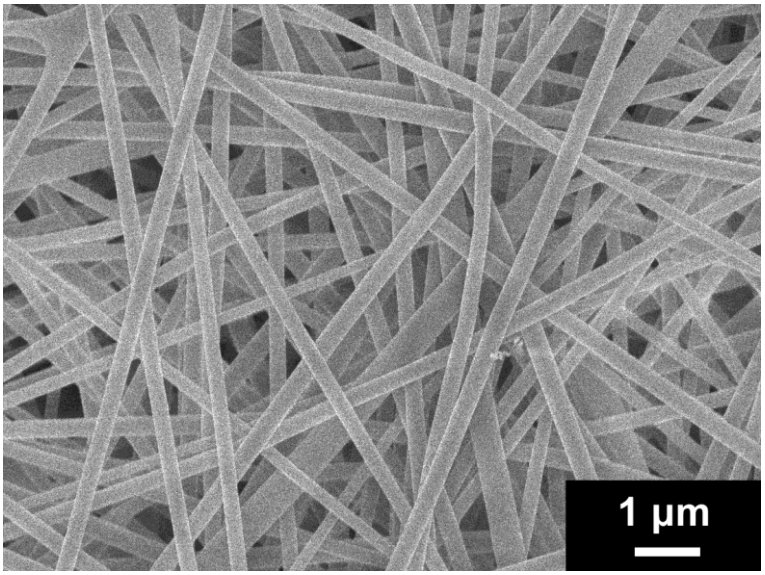

Fig. S28 FE-SEM image of **PVA** fibers prepared by an electrospinning technique

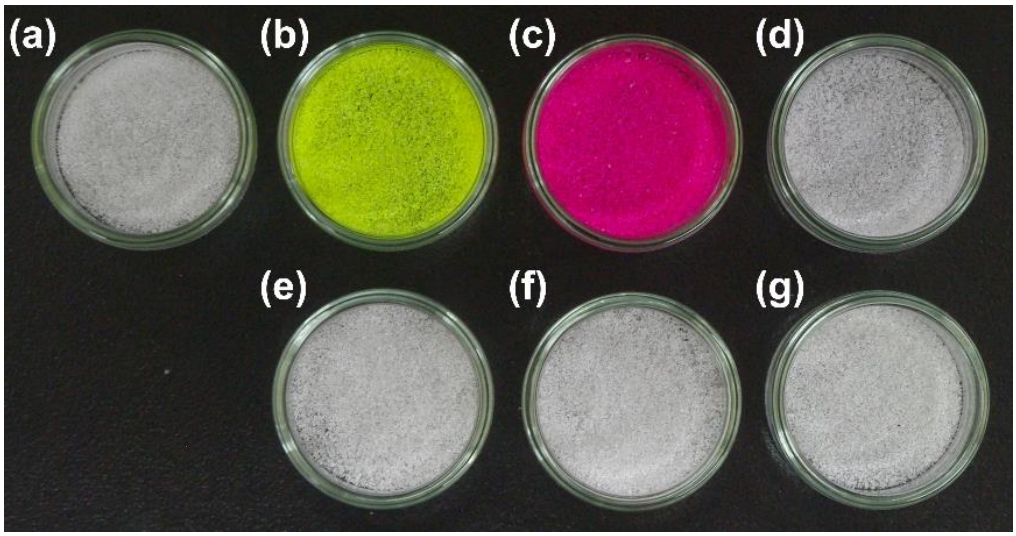

Fig. S29 Photographs of **PVA** microparticles before (a) and after the treatment with (b) **1a** (**PVA**/**1a**), (c) **2a** (**PVA**/**2a**), (d) **3a** (**PVA**/**3a**), (e) **1b** (**PVA**/**1b**), (f) **2b** (**PVA**/**2b**), (g) **3b** (**PVA**/**3b**) in petri dishes under ambient light.

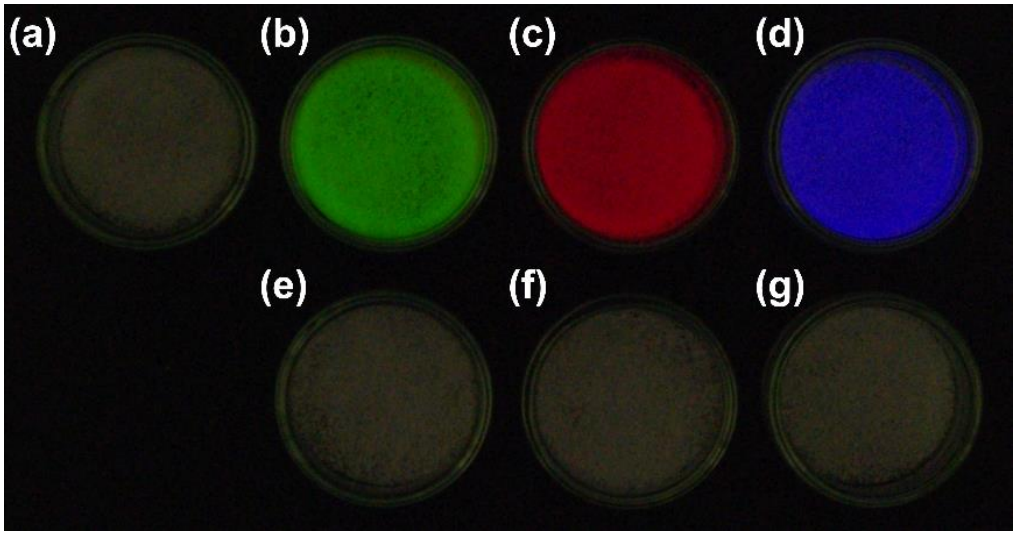

Fig. S30 Photographs of **PVA** microparticles before (a) and after the treatment with (b) **1a** (**PVA/1a**), (c) **2a** (**PVA/2a**), (d) **3a** (**PVA/3a**), (e) **1b** (**PVA/1b**), (f) **2b** (**PVA/2b**), (g) **3b** (**PVA/3b**) in petri dishes under UV light. λ_{ex} = 365 nm.

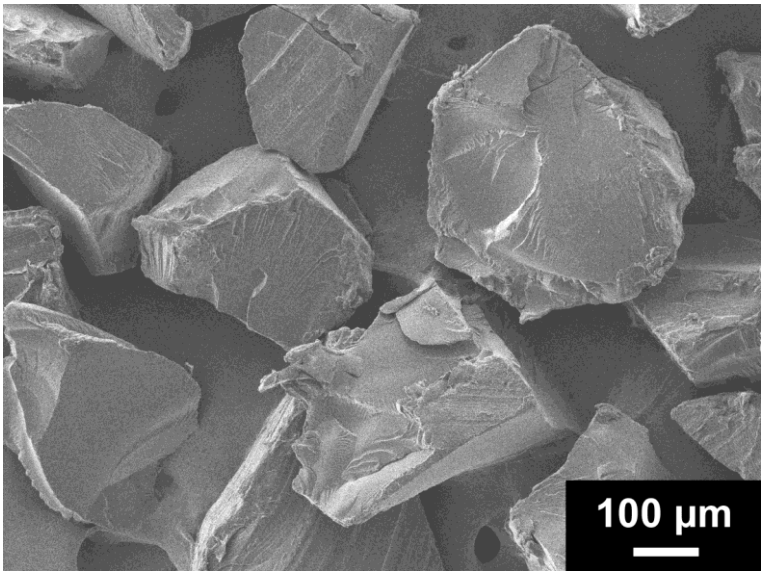

Fig. S31 FE-SEM image of **PVA/1a**.

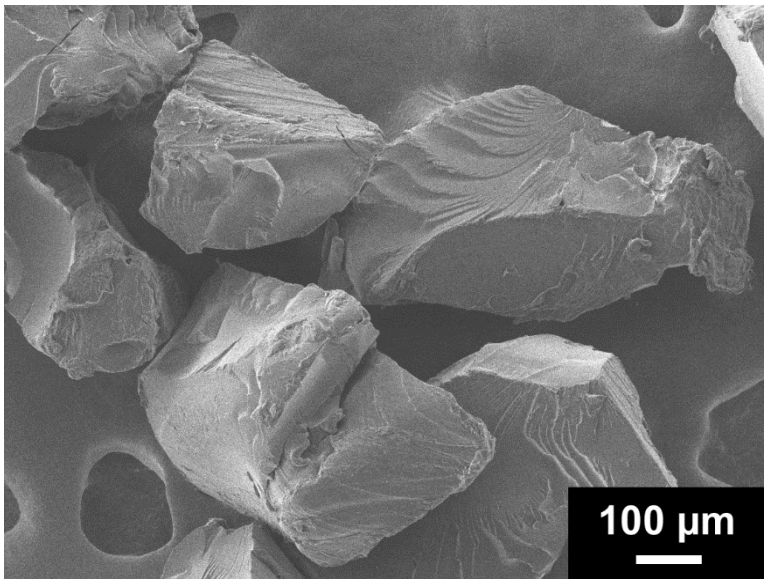

Fig. S32 FE-SEM image of **PVA/2a**.

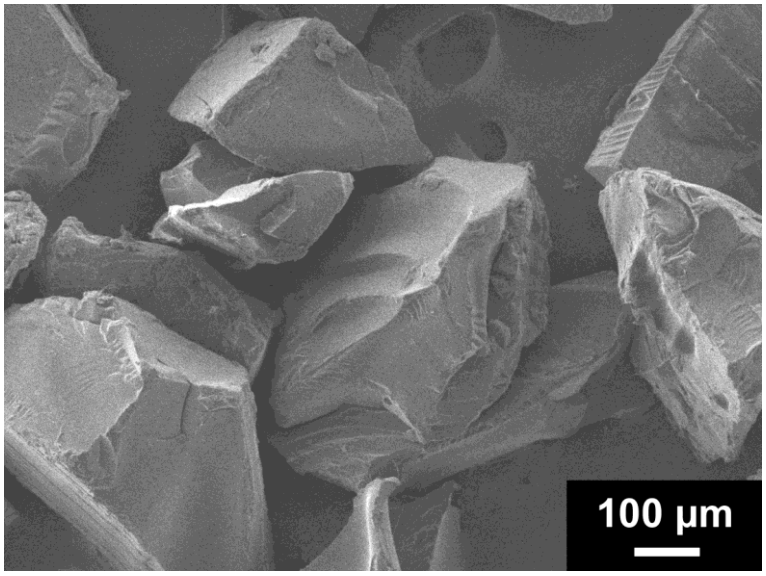

Fig. S33 FE-SEM image of **PVA/3a**.

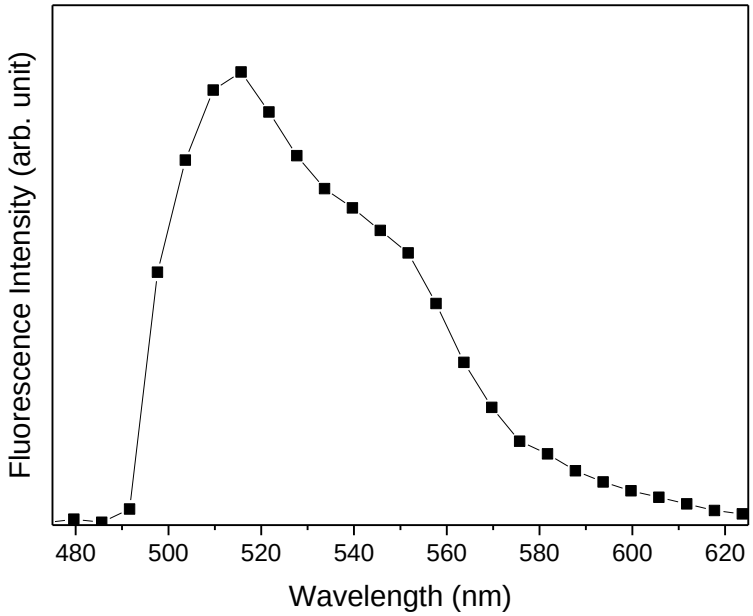

Fig. S34 Fluorescence spectrum of **PVA/1a** recorded by confocal laser scanning microscopy (λ_{ex} = 488 nm).

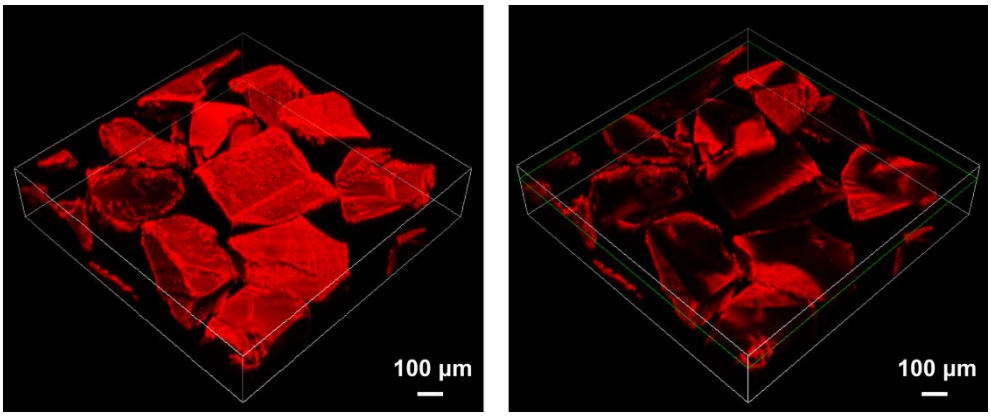

Fig. S35 Three-dimensional reconstructed fluorescence image of **PVA/2a** from confocal laser scanning microscope images (left) and a cross-sectional image confocal laser scanning microscope image at a distance of 100 μm from the top image (right). Conditions:λ_{ex} = 561 nm, λ_{em} = 570−620 nm.

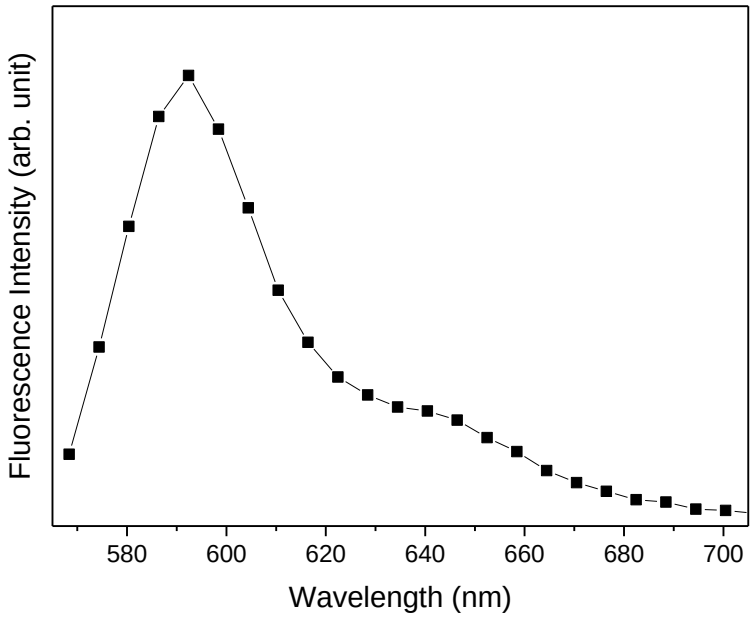

Fig. S36 Fluorescence spectrum of **PVA/2a** recorded by confocal laser scanning microscopy (λ_{ex} = 561 nm).

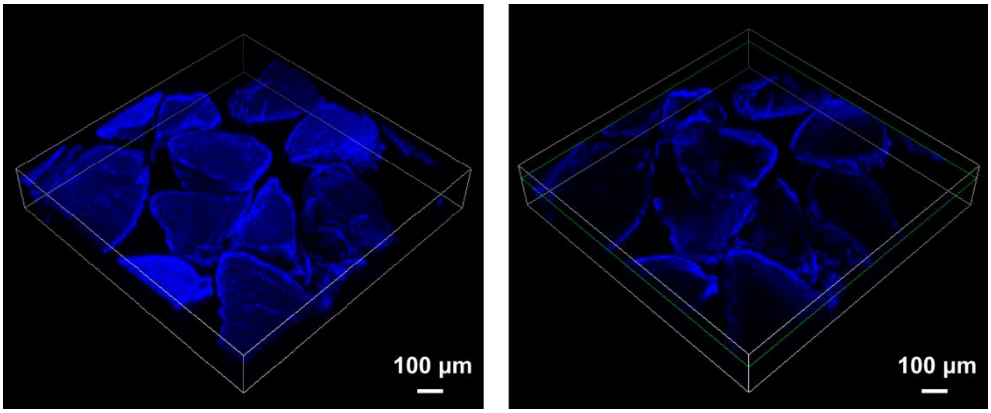

Fig. S37 Three-dimensional reconstructed fluorescence image of **PVA/3a** from confocal laser scanning microscope images (left) and a cross-sectional image confocal laser scanning microscope image at a distance of 100 μm from the top image (right). Conditions: λ_{ex} = 405 nm, λ_{em} = 425−475 nm.

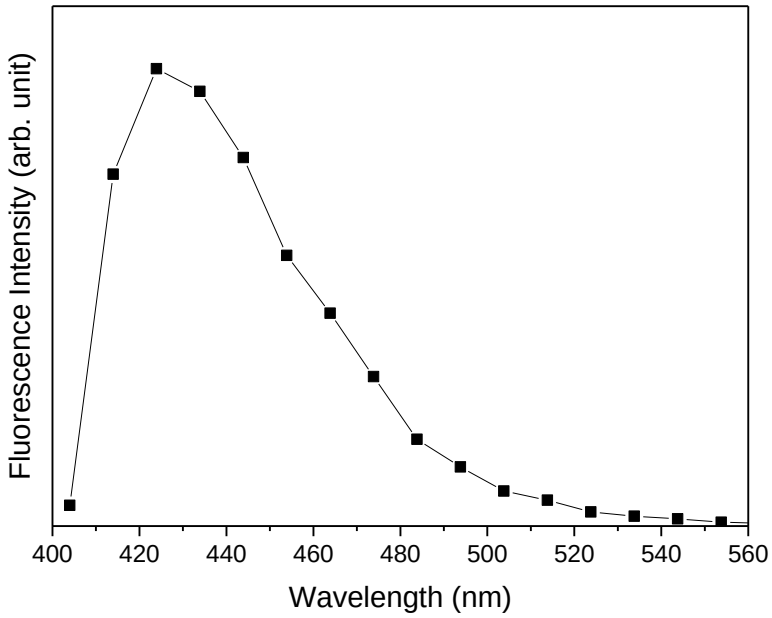

Fig. S38 Fluorescence spectrum of **PVA/3a** recorded by confocal laser scanning microscopy (λ_{ex} = 405 nm).

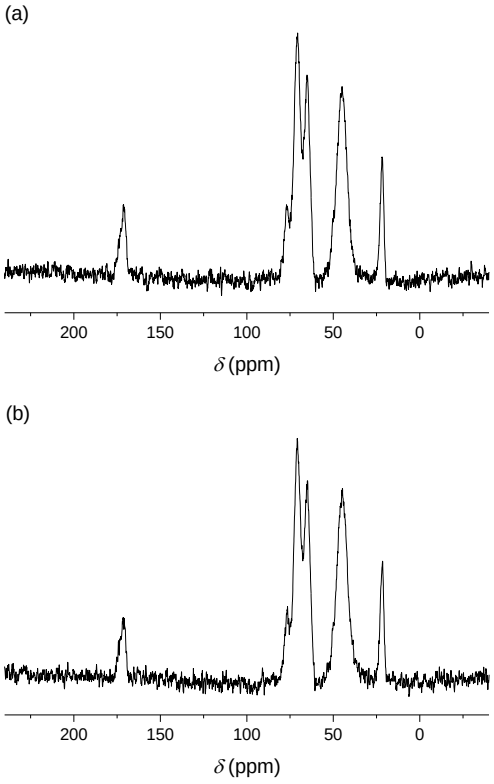

Fig. S39 Solid state ^{13}C CP MAS NMR spectra of **PVA** microparticles before (a) and after (b) the treatment with **1a**.

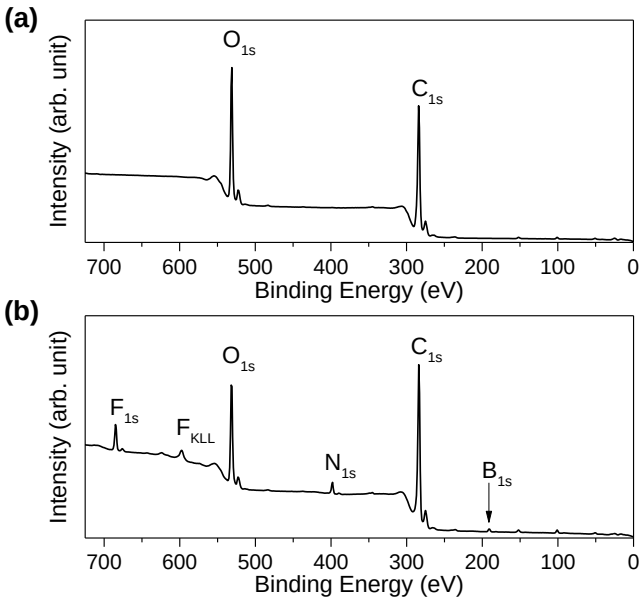

Fig. S40 XPS spectra of **PVA** microparticles (a) before and (b) after the treatment with **1a**.

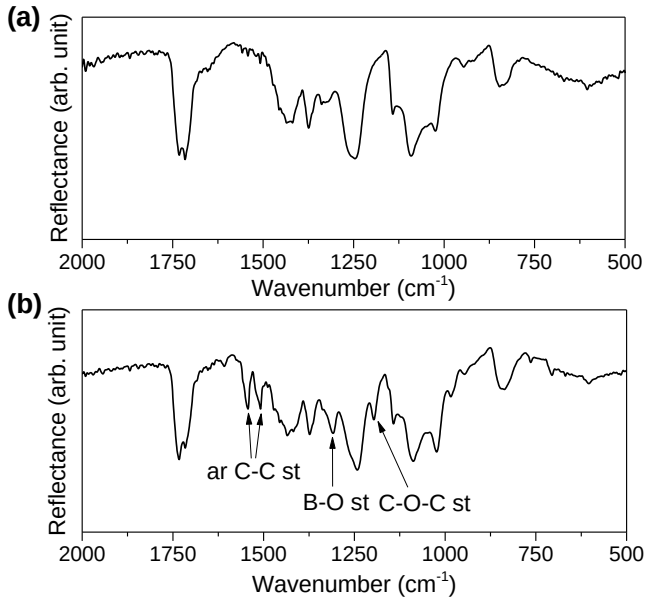

Fig. S41 ATR-FT-IR spectra of **PVA** microparticles (a) before and (b) after the treatment with **1a**.

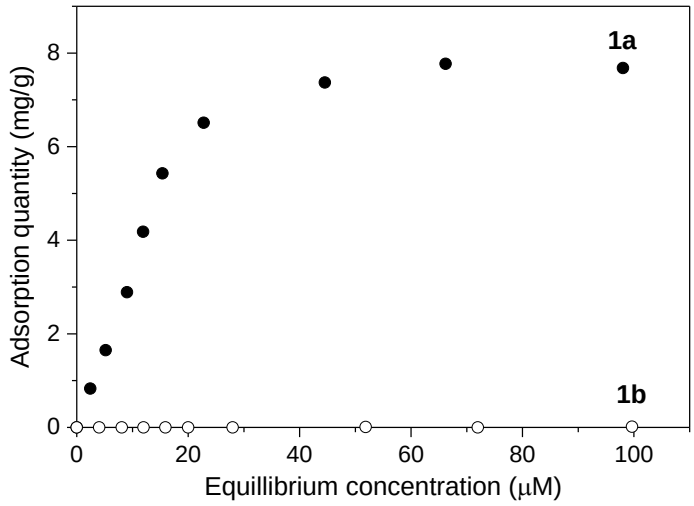

Fig. S42 Adsorption amounts of **1a** (●) and **1b** (○) to PVA microparticles at varied concentrations. **PVA** microparticles (50 mg) were immersed in methanol solutions (5.0 mL) of 1a at different concentrations at room temperature for 24 h.

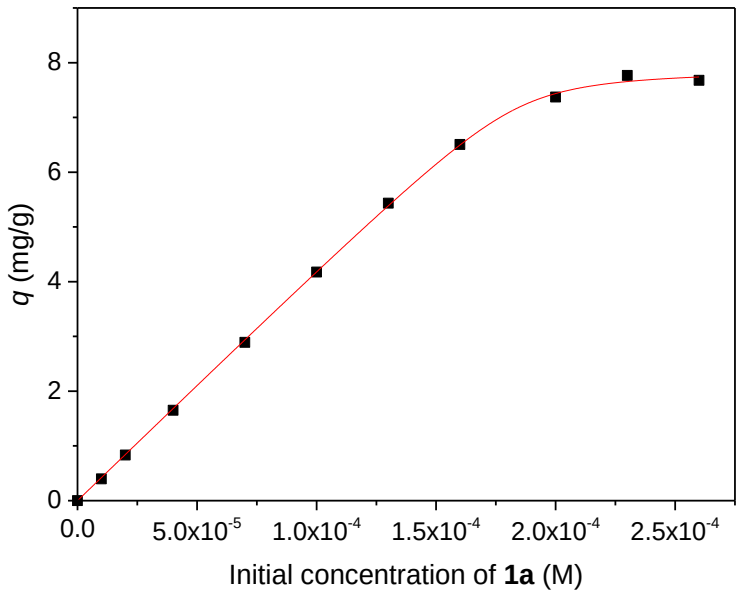

Fig. S43 Nonlinear curve fitting of an adsorption curve for adsorption of **1a** to **PVA** microparticles based on an assumption on a stoichiometric 1:1 binding of **1a** to each diol moiety of **PVA**.

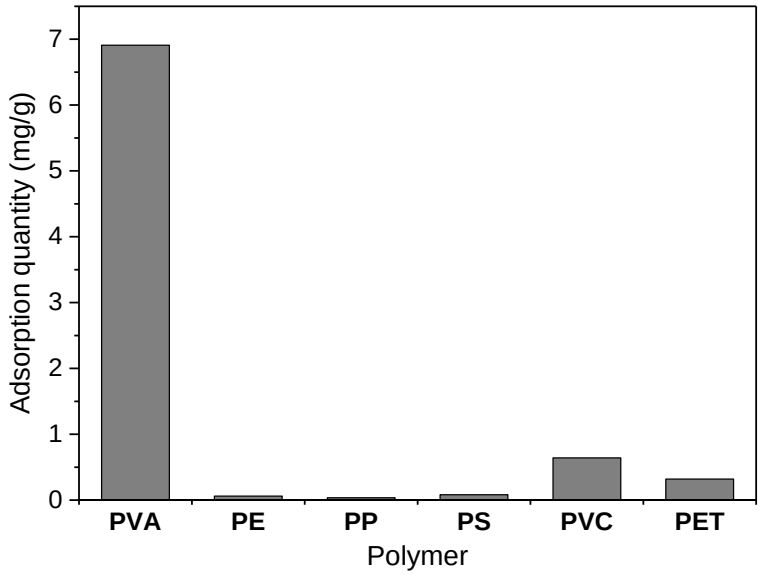

Fig. S44 Adsorption amounts of **1a** to **PVA**, polyethylene (**PE**), polypropylene (**PP**), polystyrene (**PS**), polyvinyl chloride (**PVC**) and polyethylene terephthalate (**PET**). Each polymer sample (50 mg) was immersed in a methanol solution of **1a** (2.0×10^{-4} M) at room temperature for 24 h.

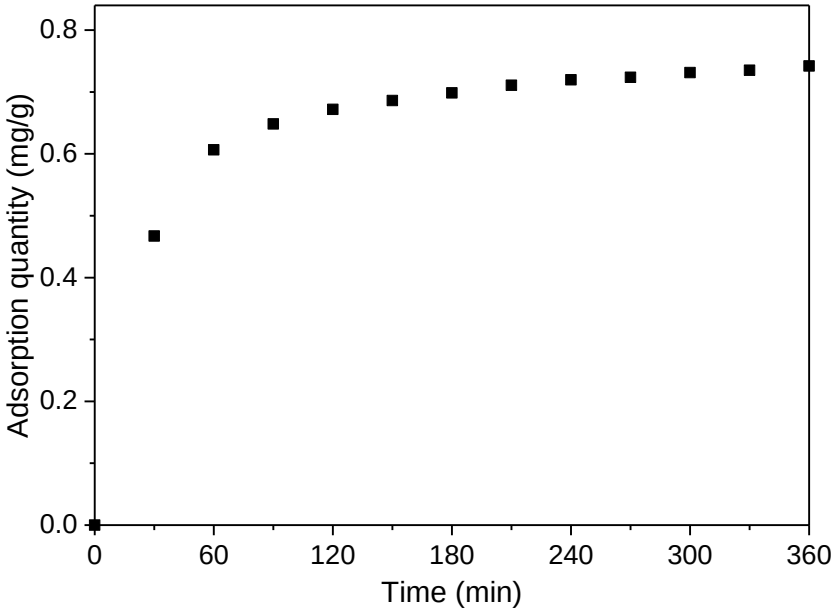

Fig. S45 Time-dependency of adsorption amounts of **1a** ([**1a**] = 2.0×10^{-5} M) to **PVA** microparticles (50 mg) in methanol at room temperature.

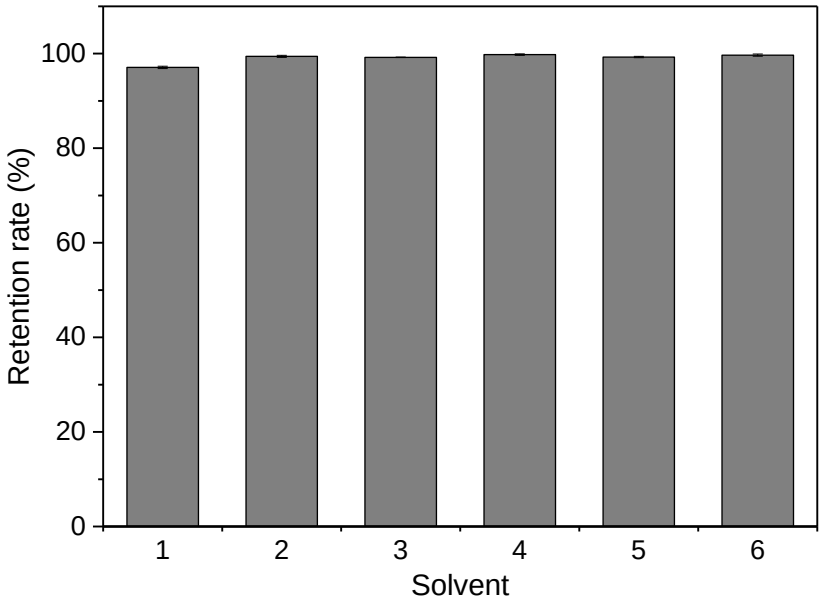

Fig. S46 Retention rates of attached **1a** onto the surface of **PVA** microparticles (**PVA**/**1a**) in organic solvents after 24 h (1: methanol, 2: acetone, 3: acetonitrile, 4: toluene, 5: dichloromethane and 6: chloroform).

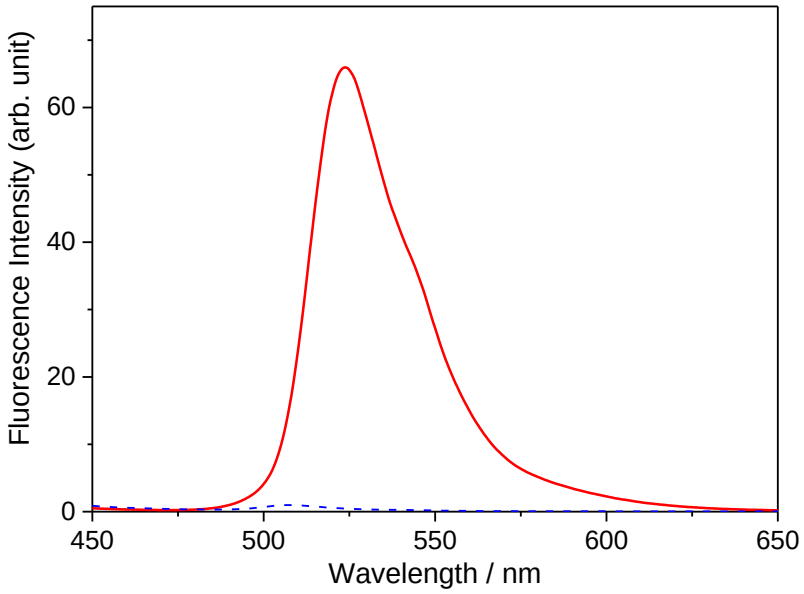

Fig. S47 Fluorescence spectra of **PVA** films treated with **1a** (solid line) and **1b** (dashed line) in methanol. λ_{ex} = 436 nm.

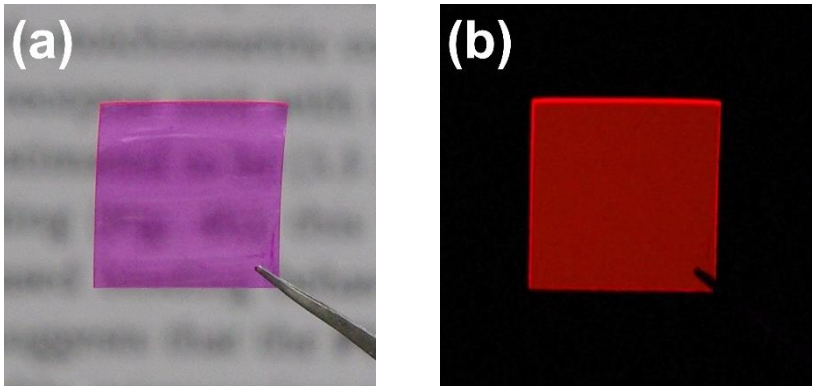

Fig. S48 Photographs of **PVA** film functionalized with **2a**. Photographs were taken under (a) ambient light and UV light (λ_{ex} =365 nm).

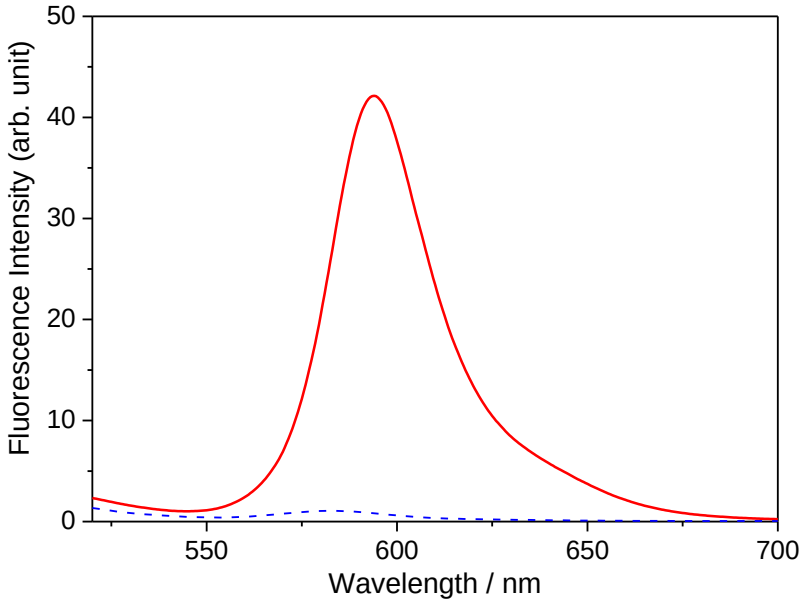

Fig. S49 Fluorescence spectra of **PVA** films treated with **2a** (solid line) and **2b** (dashed line) in methanol. λ_{ex} = 510 nm.

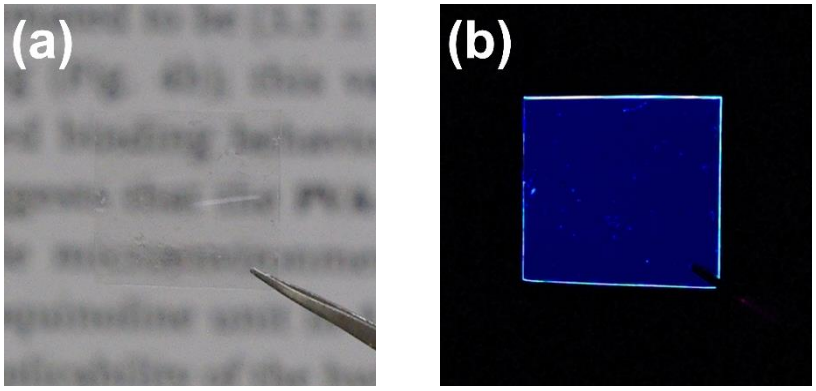

Fig. S50 Photographs of **PVA** film functionalized with **3a**. Photographs were taken under (a) ambient light and UV light (λ_{ex} =365 nm).

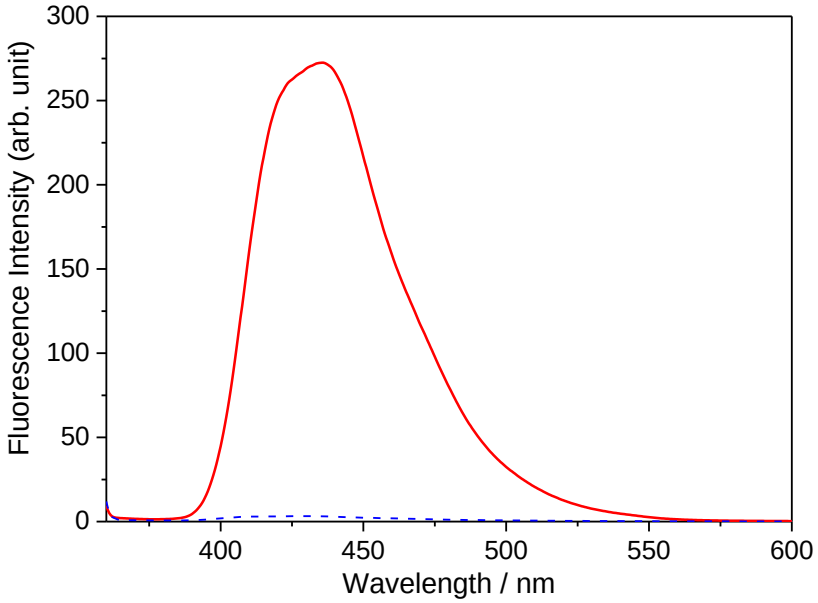

Fig. S51 Fluorescence spectra of **PVA** films treated with **3a** (solid line) and **3b** (dashed line). λ_{ex} = 355 nm.

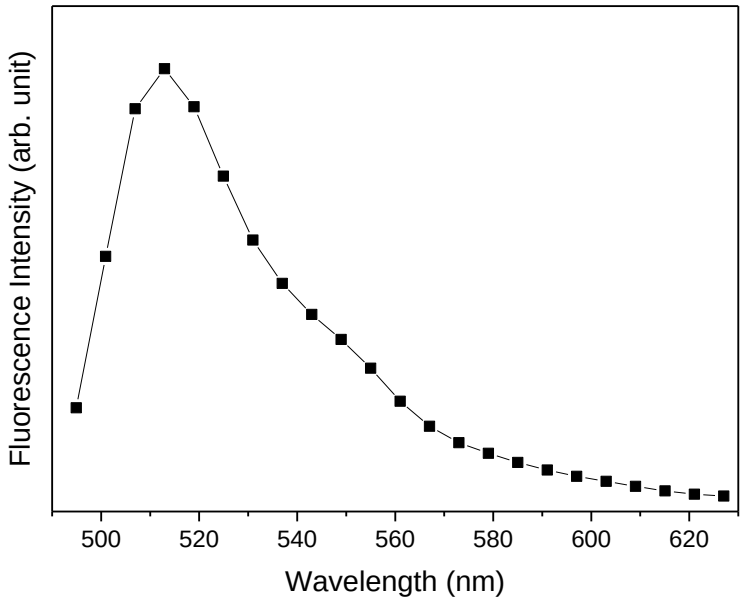

Fig. S52 Fluorescence spectrum of **PVA** nanofibers functionalized with **1a** recorded by confocal laser scanning microscopy (λ_{ex} = 488 nm).

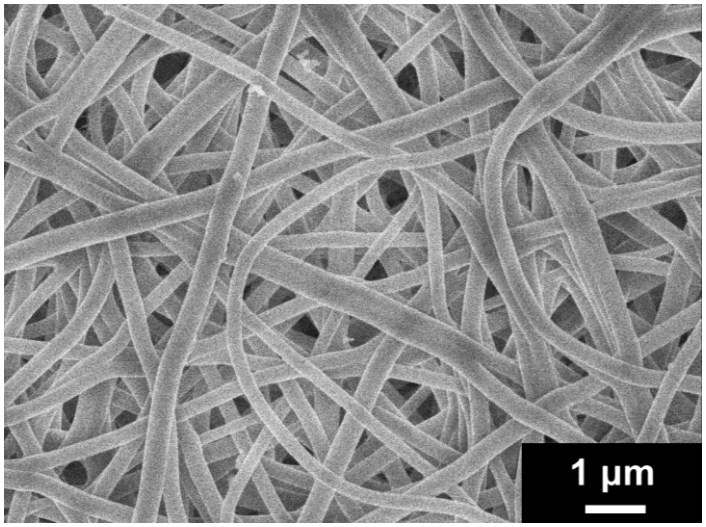

Fig. S53 FE-SEM image of **PVA** nanofibers functionalized with **2a**.

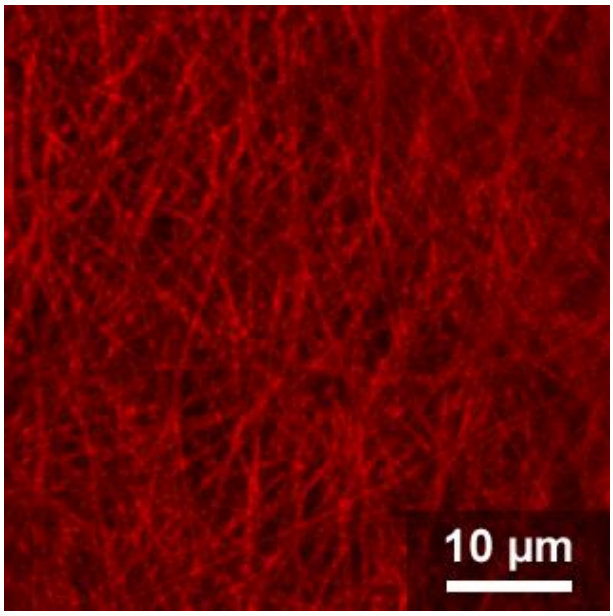

Fig. S54 Confocal laser scanning microscope fluorescence image of **PVA** nanofibers functionalized with **2a** (λ_{ex} = 561 nm, λ_{em} = 570−620 nm).

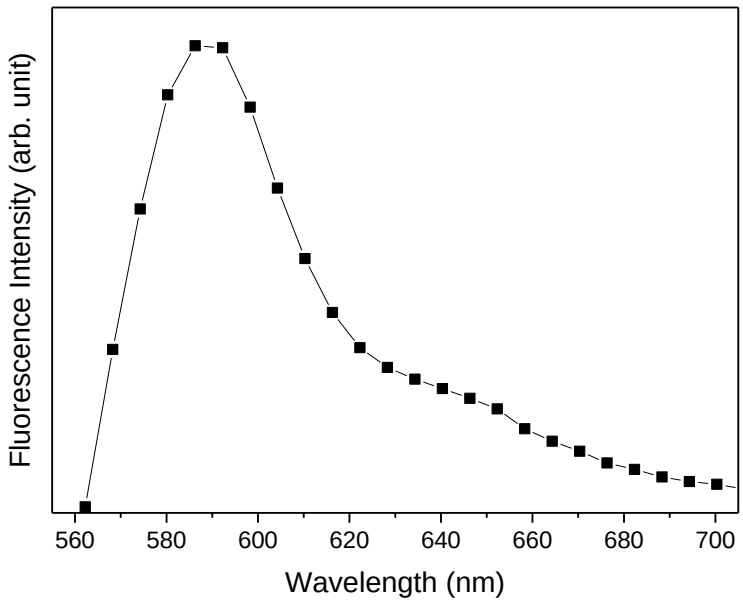

Fig. S55 Fluorescence spectrum of **PVA** fibers functionalized with **2a** recorded by confocal laser scanning microscopy (λ_{ex} = 561 nm).

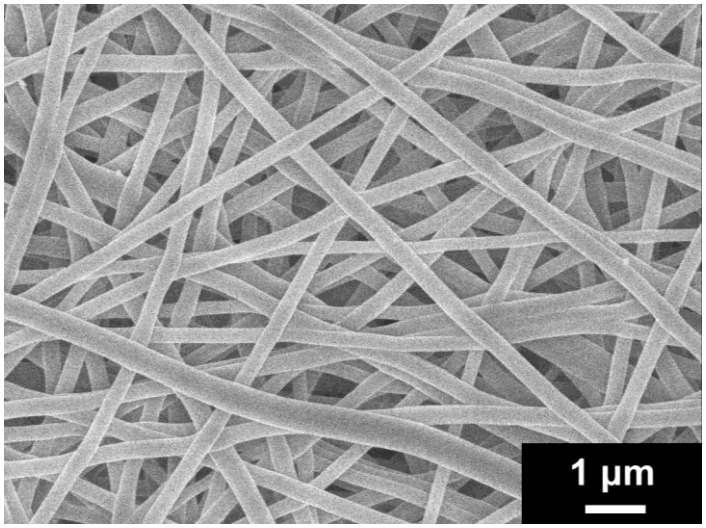

Fig. S56 FE-SEM image of **PVA** nanofibers functionalized with **3a**.

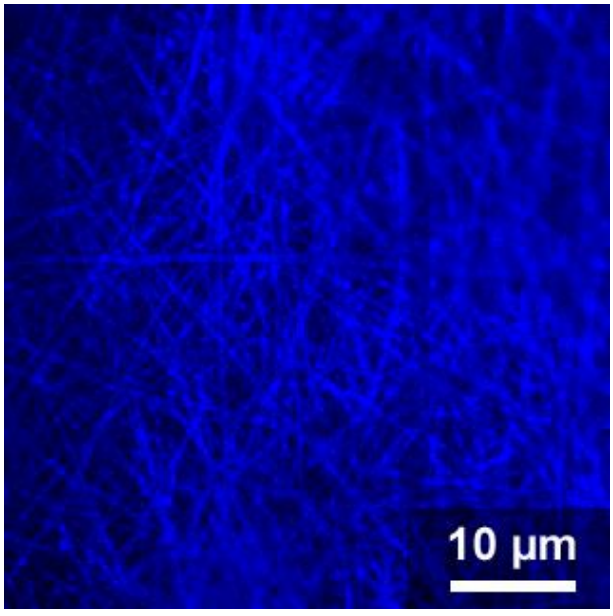

Fig. S57 Confocal laser scanning microscope fluorescence image of **PVA** nanofibers functionalized with **3a** (λ_{ex} = 405 nm, λ_{em} = 425−475 nm).

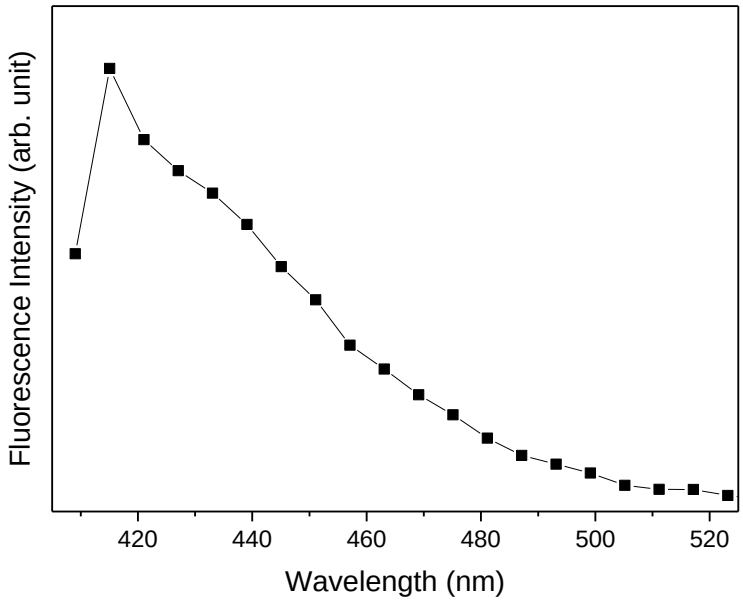

Fig. S58 Fluorescence spectrum of **PVA** fibers functionalized with **3a** recorded by confocal laser scanning microscopy (λ_{ex} = 405 nm).